waterloopkundig laboratorium
delft hydraulics laboratory

computation of density currents in estuaries

numerical accuracy of the model

report on mathematical investigation

R 897 part IV

August 1979

tow
toegepast onderzoek waterstaat

computation of density currents in estuaries

numerical accuracy of the model

report on mathematical investigation

R 897 part IV

August 1979

tow
toegepast onderzoek
waterstaat

CONTENTS

NOTATION

FIGURES

FIGURES (continued)

NOTATION

A_0, A_k	Fourier coefficients
B_0, B_k	Fourier coefficients
b	width
C	Chézy coefficient
c	concentration
$c^n_{i,j}$	discretised concentration
c_1, c_2, c_3, c_4	coefficients in special treatment near the bottom
D_x, D_z	diffusivity, in the x- and z-direction respectively
$D_{x_{ij}}, D_{z_{ij}}$	discretised diffusivities
D_{nx}	numerical diffusivity in the x-direction
E_{nx}	numerical viscosity in the x-direction
F_j	function, describing velocity boundary condition
g(t,z)	function, describing concentration boundary condition
h(t)	function, describing tidal boundary condition
H	depth
H.W.S.	high water slack
k	integer
k_1	wave number
L	length
L_i	intrusion length
L.W.S.	low water slack
L_t, L_x, L_z	displacement operators
M.E.V.	maximal ebb velocity
n	normal direction
M.F.V.	maximal flood velocity
N_t	number of time steps
N_x, N_z	number of steps in the x- and z-direction respectively
0	order symbol of Landau
p	pressure
Q	discharge
Q_r	river discharge
Q_t	tidal discharge
R	hydraulic radius
t	time
T	tidal period

NOTATION (continued)

u	velocity in the x-direction
u_0, u_t	velocity in constructed test case
u_{ij}^n	discretised velocity
u^*	shear velocity
w	velocity in the z-direction
w_{ij}^n	discretised velocity w
x	longitudinal direction
z	vertical direction
z_b	position of the bottom
z_0	coefficient for roughness length
$\Delta x, \Delta z$	step size in the x- and z-direction respectively
$\varepsilon_x, \varepsilon_z$	turbulent diffusion coefficient for momentum in the x- and z-direction respectively
κ	Von Karman coefficient
ψ	phase angle
ϕ_k	phase angle in Fourier series
ρ	density
τ	time step
ζ	position of the free surface
ζ_0	position of the free surface at x = 0
ω	frequency
ω_k	frequency in Fourier series

COMPUTATION OF DENSITY CURRENTS IN ESTUARIES

1 Introduction

The present Report is the first of a series of three in which the verification of the vertical two-dimensional density currents model DISTRO for tidal flume conditions is presented. In this Report the numerical accuracy is discussed; the second Report will deal with the verification for homogeneous conditions; and the third Report with the inhomogeneous conditions.
In the present Report firstly a complete review of the boundary conditions is given, including the discretisation.
Much attention is paid to the physical relevance of the boundary conditions, especially at the bottom. Further, the numerical behaviour is tested for a tidal flume situation, and under homogeneous conditions. The results of these tests are discussed and finally a conclusion is formulated about the numerical accuracy of the model.
This Report, drawn up by Mr. P.A.J. Perrels, is the result of a study which is incorporated in a basic research programme T.O.W. (Working Group "Stromen en transportverschijnselen") executed by Rijkswaterstaat (Public Works and Water Control Department), the Delft Hydraulics Laboratory and other research institutes.

2 Description of the mathematical model

After integration over the width, and if the shallow water approximation is made, the equations for vertical two-dimensional homogeneous currents read:

$$\frac{\partial u}{\partial t} + \frac{1}{b}\frac{\partial (bu^2)}{\partial x} + \frac{\partial uw}{\partial z} - \varepsilon_x \frac{\partial^2 u}{\partial x^2} - \frac{\partial}{\partial z}\left(\varepsilon_z \frac{\partial u}{\partial z}\right) = -g\frac{\partial \zeta}{\partial x} \tag{2.1}$$

$$\frac{\partial \zeta}{\partial t} + \frac{1}{b}\frac{\partial}{\partial x}\left\{b \int_{z_b}^{\zeta} u \, dz\right\} = 0 \tag{2.2}$$

$$\frac{1}{b}\frac{\partial (bu)}{\partial x} + \frac{\partial w}{\partial z} = 0 \tag{2.3}$$

$$\frac{\partial c}{\partial t} + \frac{1}{b}\frac{\partial (bu)}{\partial x} + \frac{\partial (wc)}{\partial z} + \frac{1}{b}\frac{\partial}{\partial x}\left(b D_x \frac{\partial c}{\partial x}\right) = 0 \tag{2.4}$$

For ε_z a mixing length approximation is employed, which reads:

$$\varepsilon_z = \kappa^2 (z + z_0)^2 \left|\frac{\partial u}{\partial z}\right| \tag{2.5}$$

in which z_0 is a measure for the roughness length.
An extended derivation of these equations can be found in [1]. In that reference also the transformation is given to handle variations in bottom and free surface topography.
The boundary conditions read:

At the bottom, $z = z_b$: $u = 0$ (2.6a)

$w = 0$ (2.6b)

$$D_x \frac{\partial c}{\partial x}\frac{\partial z_b}{\partial x} - D_z \frac{\partial c}{\partial z} = 0 \tag{2.6c}$$

At the surface, $z = \zeta$: $\frac{\partial u}{\partial z} = 0$ (2.7a)

$$D_x \frac{\partial c}{\partial x}\frac{\partial \zeta}{\partial x} - D_z \frac{\partial c}{\partial z} = 0 \tag{2.7b}$$

At the upstream end, $x = L$: $u = f(z)\, Q(t)$ (2.8a)

$c = 0$ (2.8b)

At the downstream end, $x = 0$: $\frac{\partial^2 u}{\partial x^2} = 0$ (2.9a)

$c = c_{max}\, g(t,z)$, if $u > 0$ (2.9b)

$\frac{\partial^2 c}{\partial x^2} = 0$, if $u \leq 0$ (2.9c)

$\zeta = \zeta_0(t)$ (2.9d)

3 Treatment of the bottom roughness

3.1 Description of the computations

For the derivation of a special discretisation near the bottom some computations have been made for a specially constructed test case.
The physical and numerical data for this case are:

L	=	100.65	m
H	=	.216	m
T	=	558.75	s
ε_x	=	.37	$m^2 s^{-1}$
u_0	=	.1	$m\ s^{-1}$
ω	=	.011245	s^{-1}
k_1	=	.00632	m^{-1}
κ	=	.4	
N_x	=	20	
N_z	=	20	
N_t	=	600	
τ	=	.93125	s

The boundary conditions for u are:

$$u = u_t(t,0,z) \qquad \text{at} \quad x = 0.0 \text{ m}$$

and:

$$u = u_t(t,L,z) \qquad \text{at} \quad x = L$$

In the numerical model a z_0 is used to describe the bottom roughness. The following expression yields the relation between z_0 and C in steady-state conditions:

$$C = 18 \log(\frac{12R}{33z_0})$$

in which R is the hydraulic radius.

3.2 Construction of a test case

In [1] a special treatment was given for the computation of the velocity profile near the bottom. For nearly steady circumstances this approach appeared to be accurate enough, as can be seen from the examples given in that Reference. For non-steady situations, however, as can be expected in tidal areas, this approach dit not appear very reliable [2]. Therefore the following investigation was set up. Into the equation for the conservation of momentum in the x-direction, which reads for constant width:

$$\frac{\partial u}{\partial t} + \frac{\partial u^2}{\partial x} + \frac{\partial uw}{\partial z} - \varepsilon_x \frac{\partial^2 u}{\partial x^2} - \frac{\partial}{\partial z}(\varepsilon_z \frac{\partial u}{\partial z}) = -\frac{1}{\rho}\frac{\partial p}{\partial x} \qquad (3.1)$$

a pressure distribution was substituted, for which an analytical solution of the horizontal velocity u and the vertical velocity w was known. So the numerical results for u could be compared with an analytical expression for u, to give an indication of the accuracy of the numerical method.
The pressure distribution was obtained by substituting a selected expression for u into the equation for the conservation of momentum in the x-direction (3.1) and into the continuity equation which, for constant width, reads:

$$\frac{\partial u}{\partial x} + \frac{\partial w}{\partial z} = 0 \qquad (3.2)$$

An extended derivation is given in Appendix II.

The expression for u was so selected that near the bottom it shows a behaviour with z that can be expected in practical circumstances. In Appendix I it is shown that for tidal circumstances a logarithmic behaviour may be expected near the bottom. Accordingly, the following expression for u was selected:

$$u_t = u_0 \quad \sin(\omega t + kx) \; \{\ln(\frac{z + z_0}{z_0}) - \frac{z^2}{2H^2}\} \qquad (3.3)$$

In the test of the numerical accuracy, firstly some computations were made with the same discretisation over the whole area, and thus without special treatment near the bottom.
The first one was with the boundary conditions at $z = 0$:

II5: $u = 0$ at $z = 0$; $C = 19.2\ m^{\frac{1}{2}}s^{-1}$

And the second one with the boundary condition at $z = \Delta z$

II8: $u = u_t(\Delta z)$ at $z = \Delta z$; $C = 19.2\ m^{\frac{1}{2}}s^{-1}$

The results of these computations are shown in Figure 1, where the velocity profiles from II5 and II8 are compared with u_t.
Figure 1 shows that the results of II8 are very accurate, while the results of II5 show small deviations. It also appears that these deviations are almost constant over the height. Similar computations were made for C = 29.4

IV1: $u = 0$ at $z = 0$; $C = 29.4\ m^{\frac{1}{2}}s^{-1}$

IV2: $u = u_t(\Delta z)$ at $z = \Delta z$; $C = 29.4\ m^{\frac{1}{2}}s^{-1}$

The results are shown in Figure 2. They are analogous to the results shown in Figure 1, only the deviations are greater.
The conclusions that may be drawn from this first test are:

- A straightforward numerical approach does not reproduce the velocity profiles very accurately especially not for higher C.
- The normal discretisation can reproduce the velocity profile correctly for $z \geqq \Delta z$, so the accuracy depends mainly on the discretisation of (3.1) at $z = \Delta z$.

The next question was: "Which terms of the numerical approach cause the largest errors in the approximation of the velocity profile near the bottom?"
After comparison of numerically-computed values and values computed by the substitution of (3.3) into several terms of the equation for the conservation of momentum (3.1), it appeared that the term for the vertical exchange of momentum:

$$\frac{\partial}{\partial z}\left(\varepsilon_z \frac{\partial u}{\partial z}\right) \tag{3.4}$$

causes the largest errors. This is due to the large gradients that arise in the velocity profiles near the bottom, because of this term (3.4).
Figure 3 shows the velocity profiles that arise when in the numerical model the normal discretisation of (3.4) is replaced by substituting (3.3) into (3.4). It also shows that this substitution yields an accurate velocity profile.
The conclusion of the above is that, if in the numerical model the discretisation

of the term for the vertical exchange of momentum (3.4) in the equation for the conservation of momentum in the x-direction (3.1), is replaced by a special more suitable approximation, then the model will yield accurate velocity profiles.
So the next step will be to find a better approximation for:

$$\frac{\partial}{\partial z}\left(\varepsilon_z \frac{\partial u}{\partial z}\right) \qquad (3.4)$$

near the bottom.

3.3 Special treatment near the bottom

As stated in [1], and confirmed by the computations of 2.1, application of the same discretisation near the bottom as in the rest of the field yields inaccurate results. Therefore a special approximattion of the Reynolds stress at $z = \frac{\Delta z}{2}$:

$$\varepsilon_z \frac{\partial u}{\partial z}\bigg|_{z = \frac{\Delta z}{2}}$$

has to be given to replace the usual discretisation.

Starting from the equation for the conservation of momentum in the x-direction:

$$\frac{\partial u}{\partial t} + \frac{\partial u^2}{\partial x} + \frac{\partial uw}{\partial z} - \varepsilon_x \frac{\partial^2 u}{\partial x^2} - \frac{\partial}{\partial z}\left(\varepsilon_z \frac{\partial u}{\partial z}\right) = -\frac{1}{\rho}\frac{\partial p}{\partial x} \qquad (3.1)$$

rewritting yields approximately:

$$\frac{\partial}{\partial z}\left(\varepsilon_z \frac{\partial u}{\partial z}\right) = c_1 z + c_2 \qquad 0 \leqslant z \leqslant \Delta z \qquad (3.5)$$

in which c_1 and c_2 are given by:

$$c_1 = \left[\left\{\frac{1}{\rho}\frac{\partial p}{\partial x} + \frac{\partial u}{\partial t} + \frac{\partial u^2}{\partial x} + \frac{\partial uw}{\partial z} - \varepsilon_x \frac{\partial^2 u}{\partial x^2}\right\}_{z = \Delta z} - c_2\right] / \Delta z \qquad (3.6)$$

$$c_2 = \left\{\frac{1}{\rho}\frac{\partial p}{\partial x} + \frac{\partial u}{\partial t} + \frac{\partial u^2}{\partial x} + \frac{\partial uw}{\partial z} - \varepsilon_x \frac{\partial^2 u}{\partial x^2}\right\}_{z = 0} \qquad (3.7)$$

This corresponds to an approximation of the Reynolds stress by a quadratic function of z:

$$\varepsilon_z \frac{\partial u}{\partial z} = \frac{c_1}{2} z^2 + c_2 z + c_3 \tag{3.8}$$

If a mixing length approximation is applied with

$$\varepsilon_z = \kappa^2 (z + z_0)^2 \left|\frac{\partial u}{\partial z}\right| \tag{3.9}$$

in which z_0 is a measure for the roughness length,

then substitution of (3.9) into (3.8) and rewriting yields:

$$\frac{\partial u}{\partial z} = \left\{\frac{\sqrt{\left(1+\frac{c_2}{c_3} z + \frac{c_1}{2c_3} z^2\right)}}{\kappa^2 (z + z_0)} \frac{1}{\left|\frac{\partial u}{\partial z}\right|}\right\} c_3 \frac{\sqrt{\left(1+\frac{c_2}{c_3} + \frac{c_1}{2c_3} z^2\right)}}{(z + z_0)} \tag{3.10}$$

with $\left|\frac{c}{c_3} z + \frac{c_1}{2c_3} z^2\right| < < 1 \quad \text{for} \quad 0 \leqq z \leqq \Delta z$

Now the first term on the right hand side of (3.10) is a constant:

$$c_4 = \frac{\sqrt{\left(1 + \frac{c_2}{c_3} z + \frac{c_1}{2c_3} z^2\right)}}{\kappa^2 (z + z_0)} \frac{1}{\left|\frac{\partial u}{\partial z}\right|} . \tag{3.11}$$

Developing the square root of (3.10) into a series of z yields, if higher order terms are neglected:

$$\frac{\partial u}{\partial z} = c_4 \frac{\left\{\frac{c_1}{4} z^2 + \frac{c_2}{2} z + c_3\right\}}{(z + z_0)} \tag{3.12}$$

which shows the correct behaviour of

$\frac{\partial u}{\partial z}$ for $z \to 0$.

Integration of (3.12) and substitution of the boundary conditions:

at $z = 0$: $u = 0$ (3.13)

at $z = \Delta z$: $u = u(\Delta z)$ (3.14)

yields an expression for c_3, which is linearly dependent on $u(\Delta z)$. Substitution of c_3 into (3.8) gives the desired relation from which

$$\varepsilon_z \left.\frac{\partial u}{\partial z}\right|_{z = \frac{\Delta z}{2}}$$

can be computed.

An extended derivation can be found in Appendix III.

3.4 Implementation and verification of the special treatment near the bottom

When implementing the suggestions of 3.2 into the numerical model, the discretisation of two quantities is of major importance.
In the first place it appeared during the test computation that the discretisation of $\frac{\partial u}{\partial t}$ in equation (3.6) was important, especially around H.W.S. and L.W.S. when the velocities reverse direction. A second order backward discretion of $\frac{\partial u}{\partial t}$ appeared to be accurate enough:

$$\left(\frac{\partial u}{\partial t}\right)^n = \frac{1.5\ u^n - 2.0\ u^{n-1} + 0.5\ u^{n-2}}{\tau}, \tag{3.15}$$

n denoting the time level: $t = n\tau$.

The importance of the discretisation of $|\frac{\partial u}{\partial z}|$ becomes clear from (3.10).
In fact a non-linear equation has to be solved and with an appropiate discretisation of $|\frac{\partial u}{\partial z}|$ an iteration process could be avoided.
Finally, the following approximation appeared to give satisfactory results:
For the computation of u^{n+1} an approximation of $|\frac{\partial u}{\partial z}|^{n+1}$ is needed: $|\frac{\partial u}{\partial z}|^*$, which is given by:

$$\left|\frac{\partial u}{\partial z}\right|^* = 0.5\ \{\left|\frac{\partial u}{\partial z}\right|^n + \left|\frac{\Delta u}{\Delta z}\right|^n\}, \tag{3.16}$$

in which $|\frac{\partial u}{\partial z}|^n$ is computed from (3.10) and $|\frac{\Delta u}{\Delta z}|^n$ is computed from:

$$\left|\frac{\Delta u}{\Delta z}\right|_{z = \Delta z} = \frac{A_1}{(\Delta z + z_0)} + A_2, \tag{3.17}$$

in which:

$$A_1 = \frac{2\,u(\Delta z) - u(2\Delta z)}{2\,\ln\left(\frac{\Delta z + z_0}{z_0}\right) - \ln\left(\frac{2\Delta z + z_0}{z_0}\right)} \tag{3.18}$$

$$A_2 = \frac{u(\Delta z) - A_1\,\ln\left(\frac{\Delta z + z_0}{z_0}\right)}{\Delta z} \tag{3.19}$$

This approach appeared to be sufficiently accurate to avoid an iteration process. A derivation of (3.17) to (3.19) is given in Appendix IV.

For the verification first a comparison is made between a computation with the same discretisation over the whole area and a computation with the special treatment near the bottom.

IV 2 : everywhere the same discretisation; $C = 29.4\ m^{\frac{1}{2}}s^{-1}$.

IV 29: with special treatment near the bottom; $C = 29.4\ m^{\frac{1}{2}}s^{-1}$.

In Figure 4 the results are shown together with u_t. It is evident that the special treatment near the bottom improves the accuracy considerably.
The verification was completed with a test of the dependency on the vertical stepsize: Δz. Therefore computation IV 29 was repeated with different Δz, respectively:

IV 34: Δz = .036 m
IV 35: Δz = .018 m
IV 36: Δz = .009 m

The differences appear to be in the order of the desired accuracy defined in [3], which corresponds with the differences caused by a variation of 5% in C.

A harmonic analysis of the discharges yields:

IV 34: $Q(x = 50.325\ m) = .0504 \cos(\omega t + 1.0106)$
IV 35: $Q(x = 50.325\ m) = .0511 \cos(\omega t + 1.0056)$
IV 36: $Q(x = 50.325\ m) = .0514 \cos(\omega t + 1.0043)$

Integrating u_t yields a discharge:

$$Q(x = 50.325 \text{ m}) = .0516 \cos(\omega t + 1.0018)$$

which shows the accuracy of the numerical results and a clear convergence for decreasing Δz.

4 Treatment of the other boundaries

4.1 Boundary conditions at the free surface and the bottom

At the free surface the boundary condition for the momentum equation reads:

$$\frac{\partial u}{\partial n} = 0, \qquad (4.1)$$

which means that no wind influence is considered. In its discretised form equation (4.1) is taken as:

$$u_{i,nzz} = u_{i,nzz-1}, \qquad (4.2)$$

which implies:

$$\frac{\partial u}{\partial z} = 0. \qquad (4.3)$$

Appendix V gives an account of this approach.

The boundary condition for the diffusion equation reads at the free surface:

$$D_x \frac{\partial c}{\partial x} \frac{\partial \zeta}{\partial x} - D_z \frac{\partial c}{\partial z} = 0, \qquad (4.4)$$

which means that the flux of dissolved matter through the free surface is zero.

In its discretised form this boundary condition reads:

$$D_{x_{i,nzz}} \frac{(c^n_{i+1,nzz} - c^n_{i-1,nzz})}{2\ \Delta x} \frac{(\zeta^n_{i+1} - \zeta^n_{i-1})}{2\ \Delta x} - D_{z_{i,nzz}} \frac{(c^{n+1}_{i,nzz} - c^{n+1}_{i,nzz-1})}{\Delta z} = 0 \qquad (4.5)$$

At the bottom a similar condition for the diffusion equation exists, which reads:

$$D_x \frac{\partial c}{\partial x} \frac{\partial z_b}{\partial x} - D_z \frac{\partial c}{\partial z} = 0.$$

In its discretised form (4.6) reads: (4.6)

$$D_{x_{i,1}} \frac{(c^n_{i+1,1} - c^n_{i-1,1})}{2\,\Delta x} \frac{(z^n_{b_{i+1}} - z^n_{b_{i-1}})}{2\,\Delta x} \frac{(c^{n+1}_{i,2} - c^{n+1}_{i,1})}{\Delta z} = 0 \qquad (4.7)$$

The boundary condition for the momentum equation at the bottom reads:

$$u = 0. \qquad (4.8)$$

4.2 Boundary conditions at the upstream boundary

At the upstream boundary the discharge must be given in combination with a velocity profile. The discharge can be specified as a Fourier-series in which not only are the amplitudes important, but also the phase. Especially the phase-difference with the downstream boundary appeared to be very critical [3].

In its discretised form this boundary condition reads:

$$u_{nxx,j} = F_j \{A_0 + \sum_{k=1}^{K} A_k \cos(kt\omega - \phi_k)\}. \qquad (4.9)$$

With regard to the upstream boundary condition of the diffusion equation it is supposed that the concentration is zero. In terms of salt content this means that the salt wedge does not reach the upstream boundary.
The discretised boundary condition reads:

$$c_{nxx,j} = 0 \qquad (4.10)$$

4.3 Boundary conditions at the downstream boundary

At the downstream boundary in the first place the position of the free surface must be prescribed as a function of time:

$$\zeta = \zeta_0(t) \qquad (4.11)$$

This condition introduces the tidal oscillations into the model, and after discretisation it reads:

$$\zeta^n_0 = B_0 + \sum_{k=1}^{K} B_k \cos(kt\omega - \phi_k). \qquad (4.12)$$

Further, a boundary condition for the momentum equation must be given. From a mathematical point of view prescribing the velocity profile should be a correct boundary condition; in practice, however, this cannot be realized. Therefore the following weak condition is adopted, which leaves the velocities free to settle:

$$\frac{\partial^2 u}{\partial x^2} = 0. \tag{4.13}$$

Straightforward discretisation of (4.13) would mean an extrapolation over the first grid step, and nothing of the physical processes would be included. Therefore (4.13) is substituted into the momentum equation (3.1), which then reduces to:

$$\frac{\partial u}{\partial t} + \frac{\partial u^2}{\partial x} + \frac{\partial uw}{\partial z} - \frac{\partial}{\partial z}(\varepsilon_z \frac{\partial u}{\partial z}) = -\frac{1}{\rho}\frac{\partial p}{\partial x} \tag{4.14}$$

Next (4.14) is split according to the normal splitting technique. For the discretisation of the part in the x-direction a one-sided second order difference scheme is applied.

The difference equations read:

$$\frac{u^*_{nxx,j} - u^n_{nxx,j}}{\tau} - \frac{(\frac{11}{6} u^{n^2}_{nxx,j} - 3\, u^{n^2}_{nxx-1,j} + \frac{3}{2}\, u^{n^2}_{nxx-2,j} - \frac{1}{3}\, u^{n^2}_{nxx-3,j})}{\Delta x} +$$

$$- \frac{1}{\rho^n_{nxx,j}} \frac{(1.5 p^n_{nxx,j} - 2.0 p^n_{nxx-1,j} + 0.5 p^n_{nxx-2,j})}{\Delta x} +$$

$$\frac{u^{n+1}_{nxx,j} - u^*_{nxx,j}}{\tau} - \frac{(w^n_{nxx,j+1} u^{n+1}_{nxx,j+1} - w^n_{nxx,j-1} u^{n+1}_{nxx,j-1})}{2\,\Delta z}$$

$$+ \{\frac{\varepsilon^n_{z\,nxx,j+\frac{1}{2}}(\frac{u^{n+1}_{nxx,j+1} - u^{n+1}_{nxx,j}}{\Delta z}) - \varepsilon^n_{z\,nxx,j-\frac{1}{2}}(\frac{u^{n+1}_{nxx,j} - u^{n+1}_{nxx,j-1}}{\Delta z})}{\Delta z}\} \tag{4.15}$$

Finally, a boundary condition must be given for the diffusion equation. For this condition the same arguments hold as for the boundary condition of the momentum equation.
In this case a combination of boundary conditions is adopted. If the velocity is directed inwards the concentration is prescribed as a function of t and z. In fact, the concentration at each level z increases linearly with time upto a maximal concentration, the concentration in the sea:

$$c = c_{max}\, g(t,z), \quad \text{if} \quad u > 0 \quad \text{(flood tide)} \tag{4.16}$$

If the velocity is directed outwards a weak boundary condition is adopted analogous to that for the velocity:

$$\frac{\partial^2 c}{\partial x^2} = 0. \tag{4.17}$$

The discretisation of (4.17) is performed analogous to the discretisation of (4.13).
In Appendix VII the truncation error and the numerical viscosity are given.

5 Accuracy

5.1 Description of the computation

To test the influence of the numerical parameters Δz, Δx and τ, a test series was set up. In that series variations in the different step sizes have been made, starting from a reference situation. The data for this reference situation, which approximates the tidal flume circumstances [3], are:

$L = 96.98 \quad m$

$H = .216 \quad m$

$T = 558.75 \quad s$

$Q_r = .0029 \quad m^3 s^{-1}$

$\varepsilon_x = .37 \quad m^2 s^{-1}$

$D_x = 2\bar{u}^* b + .005 \quad m^2 s^{-1}$

$N_x = 13$

$N_z = 12$

$N_t = 1200$

$\tau = 1.8625 \quad s$

$C = 22.3 \quad m^{\frac{1}{2}} s^{-1}$ (in the first 63.41 m)

$\quad = 24.0 \quad m^{\frac{1}{2}} s^{-1}$ (in the last 33.57 m)

The boundary condition for ξ at x = 0.0 m reads:

$$\zeta(t,0) = .2160 + .02425 \cos(\omega t)$$

The boundary condition for Q_t at x = L reads:

$$\begin{aligned} Q(t,L) = .0029 &+ .01470 \cos(\omega t + 1.3525) \\ &+ .00315 \cos(2\omega t + 3.1751) \\ &+ .00173 \cos(3\omega t + 1.9864) \\ &+ .00093 \cos(4\omega t + 4.0749) \\ &+ .00010 \cos(5\omega t + 2.0980) \\ &+ .00016 \cos(6\omega t + 3.6467) \\ &+ .00006 \cos(7\omega t + 3.2067) \\ &+ .00018 \cos(8\omega t + 4.4373) \end{aligned}$$

5.2 Influence of Δz

To test the influence of Δz on the computations, the following three runs have been made:

RB 21: $\Delta z = .036$ m ($N_z = 6$)
RB 19: $\Delta z = .018$ m ($N_z = 12$)
RB 22: $\Delta z = .009$ m ($N_z = 24$)

In Figure 5 the position of the free surface at x = L is shown. Position x = L was selected because it is the farthest away from the point where the boundary condition for the free surface is imposed.
For the same reason the influence on the velocity is shown at position: x = 0.0 m. Similar to the verification in 3.4, the differences between the various computations become smaller than the permitted differences, defined in [3]. Further, a smaller Δz yields a smaller damping and a small phase shift, as can be seen from the harmonic analysis of the motion of the free surface at x = L and of the discharges at x = 0.0 m.

RB 21: $\zeta(L) = .2219 + .0262 \cos(\omega t + 2.909)$
$Q(0) = .0029 + .0284 \cos(\omega t - 2.048)$
RB 19: $\zeta(L) = .2220 + .0272 \cos(\omega t + 2.916)$
$Q(0) = .0029 + .0290 \cos(\omega t - 2.042)$
RB 22: $\zeta(L) = .2219 + .0275 \cos(\omega t + 2.896)$
$Q(0) = .0029 + .0291 \cos(\omega t - 2.047)$

It turns out that the variations in the phase are not monotone. This is mainly due to the discretisation of the boundary condition at x = L: Q(t,L), which becomes more inaccurate for larger Δz.

The results of the harmonic analysis are confirmed by the Figures. In Figure 5 the position of the free surface is shown at x = L. It appears that the main differences occur around L.W.S. and H.W.S. Further, the differences between the computations with $\Delta z = .009$ m and $\Delta z = .018$ m are much smaller than the differences between $\Delta z = .018$ m and $\Delta z = .036$ m. The same holds for the differences in the velocity profiles at M.E.V. and M.F.V. respectively. The velocity profiles are shown in Figure 6, while Figure 7 shows the discharges at x = 0.0 m. Here the main differences occur also for $\Delta z = .036$ m, but now just after M.F.V. and M.E.V.

The influence of the vertical step size Δz on the rhodamine concentration is a direct one via the accuracy and an indirect one via the influence of Δz on the velocities. In the present tests only the integrated effect has been considered. Figure 8 shows the influence of Δz on the evolution of the depth-averaged concentrations at x = 0.0 m and at x = 14.94 m. The main differences occur during ebb tide, which corresponds with the differences in the discharge at M.F.V. (see Figure 7). A smaller Δz yields a larger flood velocity, which in turn gives higher rhodamine concentrations upstream.
The very small differences in the concentrations at x = 0.0 m during flood tide are also caused by the transition function, which was the same for all three computations.
Figures 9 and 10 show the same picture: almost identical concentrations during flood tide, and small differences in the concentrations computed with the largest grid step.
In Figure 11 the maximal concentrations occurring at x = 7.46 m are shown. The lowest concentration occurs for the largest Δz, due to the smaller velocities that occur for larger Δz. Finally, the intrusion length and the horizontal rhodamine distribution are shown in Table II.
The influence of Δz on the intrusion length is rather small. There is, however, some influence on the horizontal rhodamine distribution that has a steeper descent at its upstream side (see Table II). Summarising the influence of Δz, it may be concluded that Δz influences the tidal movement and that from the viewpoint of accuracy 24 steps in the vertical yield a good discretisation, with 12 steps as a reasonable minimum.

5.3 Influence of Δx

The size of the horizontal step size Δx influences the solution via the accuracy and via the numerical diffusivity and viscosity.
The influence of Δx is tested in the following computations:

RB 17: Δx = 7.46 m (N_x = 13)
RB 18: Δx = 3.73 m (N_x = 26)
RB 25: Δx = 1.865 m (N_x = 52).

In Figure 12 the influence of Δx on the position of the free surface is shown. This influence is very small, compared with the influence of Δz. This is confirmed by the harmonic analysis:

RB 17: $\zeta(L) = .2216 + .0268 \cos(\omega t + 2.848)$
RB 18: $\zeta(L) = .2217 + .0266 \cos(\omega t + 2.852)$
RB 25: $\zeta(L) = .2217 + .0266 \cos(\omega t + 2.852)$

Figure 13 shows the influence of Δx on the discharges and Figure 14 shows the influence on the velocity at $x = 0.0$ m during M.E.V. and M.F.V.
For the velocities, too, the influence is very small, as can be seen from a harmonic analysis of the discharges at $x = 0.0$ m:

RB 17: $Q(0) = .0029 + .0289 \cos(\omega t - 2.070)$
RB 18: $Q(0) = .0029 + .0289 \cos(\omega t - 2.068)$
RB 25: $Q(0) = .0029 + .0289 \cos(\omega t - 2.068)$

This small influence could be expected, considering the tidal wave length:

$$L_T = \sqrt{(gh)}T \approx 800 \text{ m} \tag{5.1}$$

which means that even for the largest grid-size, $\Delta x = 7.46$ m, there are more than 100 grid-points at a wave length. This is more than enough to guarantee an accurate representation of the tidal phenomena.
An estimation of the numerical viscosity [4]:

$$E_{nx} = -\frac{\tau}{8}\{16u^2 - 32\,\varepsilon_x \frac{\partial u}{\partial x}\} \tag{5.2}$$

shows that this is independent of Δx and therefore will not influence the numerical results.

The influence of Δx on the concentration of rhodamine is found to be more distinct than the influence on the velocities. This can be explained by the contribution of the turbulent diffusivity in the x-direction which is of greater importance for the transport of rhodamine than the turbulent viscosity for the transport of momentum [5]. This also makes the influence of the numerical diffusivity more important.

An estimation of the order of magnitude of the numerical diffusivity:

$$D_{nx} = -\frac{\tau}{4}\{u^2 - D_x \frac{\partial u}{\partial x}\} - \frac{\Delta x^2}{2} \frac{\partial u}{\partial x} \qquad 0 \leqq x < 2\,\Delta x \tag{5.3}$$

$$D_{nx} = -\frac{\tau}{4}\{u^2 - D_x \frac{\partial u}{\partial x}\} - \qquad 2\,\Delta x \leqq x \leqq L \tag{5.4}$$

yields:

$$|D_{nx}| \approx .02\,\tau + .0014\,\Delta x^2 \qquad 0 \leqq x < 2\,\Delta x \tag{5.5}$$

$$|D_{nx}| \approx .02\,\tau \qquad 2\,\Delta x \leqq x \leqq L \tag{5.6}$$

with a physical diffusivity in the x-direction:

$$D_x = 2|u^*|b + .005 \tag{5.7}$$

which has an order of magnitude:

$$D_x \approx .07\ m^2 s^{-1}. \tag{5.8}$$

This means that if $\Delta x \geqq 7$ m, then the numerical diffusivity will be of the same order as or larger than the physical diffusivity and can influence the results in cases where the contribution of the horizontal diffusifity is significant.
In Figure 15 the influence of Δx on the depth averaged concentrations at x = 0.0 m and at x = 14.92 m is shown. At x = 0.0 m there is a constant difference during flood time between the results with the largest Δx and the other two. This difference is due to the different build-up during ebb tide by the numerical diffusivity. The difference is kept constant during flood tide by the form of the boundary condition. At x = 14.92 m the influence of Δx is even more clear. Here the numerical diffusivity yields extra diffusion which results in a stronger damping of the depth averaged rhodamine concentrations. This behaviour of the depth averaged concentration at x = 14.92 m in Figure 15 can be explained by the opposite sign of $\frac{\partial u}{\partial x}$ in (4.3) during flood and during ebb tide.
During flood time D_{nx} is reduced, and the concentration, and thus the transport, remains somewhat smaller for larger Δx. During ebb tide, when D_{nx} is enlarged by the term with $\frac{\partial u}{\partial x}$, the opposite happens and the concentrations become larger for larger Δx.

In Figure 16 and 17 the influence of Δx on the concentration profiles at $x = 0.0$ m at M.F.V. and M.E.V. respectively are shown. The differences at M.F.V. are very small, but at M.E.V. there appears to be a noticeable difference, which is still, however, less than two percent of c_{max}. These differences agree very well with the results shown in Figure 15 at $x = 0.0$ m.
Figure 18 shows the influence of Δx on the maximal concentration at $x = 7.46$ m. The influence is only of the order of one percent of c_{max}.

Table II shows that during maximal intrusion the concentrations increase with Δx, particularly at large x. The intrusion length also increase for larger Δx. This effect, too, is due to the numerical diffusivity.

Summarsing the influence of Δx, it may be concluded, that this influence manifests itself mainly via the numerical diffusivity.
For an accurate computation of the concentration it is, therefore, necessary to choose $\Delta x \leqslant 2.0$ m. This holds, of course, only for the tidal flume circumstances described in (5.1). Another geometry would permit other discretisations. For the tidal movement alone, without concentrations, much larger sizes of Δx would still give accurate results.

5.4 Influence of the time step τ

The time step τ influences the computations, analogous to the step size Δx, via the accuracy and via the numerical viscosity and diffusivity.
To test the influence of τ the following computations have been made:

RB 16: $\tau = 1.8625$ s
RB 17: $\tau = .93125$ s
RB 24: $\tau = .465625$ s

The influence of τ on the position of the free surface is comparable with the influence of Δx. The harmonic analysis of the motion of the free surface is given by:

RB 16: $\zeta(L) = .22163 + .0266 \cos(\omega t + 2.829)$
RB 17: $\zeta(L) = .22164 + .0268 \cos(\omega t + 2.852)$
RB 24: $\zeta(L) = .22169 + .0268 \cos(\omega t + 2.854)$

That the influence of τ on the position of the free surface is very small could be expected considering the number of time steps per tidal period, which even for the greatest time step is still 300. The same arguments hold for the velocities and the discharges.

The influence of τ on the discharge and the velocities at x = 0.0 m appears clearly from a harmonic analysis of the discharges at x = 0.0; which shows that the influence is small.

RB 16: $Q(0) = .0029 + .0289 \cos(\omega t - 2.073)$
RB 17: $Q(0) = .0029 + .0289 \cos(\omega t - 2.070)$
RB 24: $Q(0) = .0029 + .0289 \cos(\omega t - 2.070)$

The influence of τ on the concentrations is of about the same order as the influence of Δx, as can be concluded from the expressions for the numerical diffusivity:

$$D_{nx} = -\frac{\tau}{4}\{u^2 - D_x \frac{\partial u}{\partial x}\} - \frac{\Delta x^2}{2} \frac{\partial u}{\partial x} \qquad 0 \leqq x < 2\,\Delta x \qquad (5.3)$$

$$D_{nx} = -\frac{\tau}{4}\{u^2 - D_x \frac{\partial u}{\partial x}\} \qquad 2\,\Delta x \leqq x \leqq L \qquad (5.4)$$

The orders of magnitude are given by:

$$|D_{nz}| \approx .02\,\tau + .0014\,\Delta x^2 \qquad 0 \leqq x < 2\,\Delta x \qquad (3.5)$$

$$|D_{nz}| \approx .02\,\tau \qquad 2\,\Delta x \leqq x \leqq L \qquad (3.6)$$

with a physical diffusivity of an order of:

$$D_x \approx .07\ m^2 s^{-1}. \qquad (5.8)$$

This means that $\tau = 1.88$ yields a numerical diffusivity of 40% of the physical diffusivity D_x. However the influence of τ on the numerical diffusivity will always be in one direction, because always $u^2 - D_x \frac{\partial u}{\partial x} > 0$, whereas the influence of Δx^2 changes direction with the sign of $\frac{\partial u}{\partial x}$.

This is clearly seen in Figure 19, where a smaller τ yields higher concentrations over the whole field and through the whole tidal period.
This behaviour is confirmed by Figures 20 and 21 which show the concentration profile at $x = 0.0$ m by M.F.V. and M.E.V. respectively, and also by Figure 22 where the maximal concentration at $x = 7.46$ m is shown.
The magnitude of τ has only little effect on the intrusion length, as appears clearly from Table II.

For the influence of τ similar conclusions hold as for Δx. For the time step this means that for accurate computations of the concentrations $\tau \leqslant .25$ should hold. For the tidal movement alone again much larger time steps are allowed. In contrast to Δx it is, however, not necessary to compute the tide and the concentrations with the same τ. So the time step for the tidal computation will be fixed by stability and the time step for the computation of the concentration will be fixed by numerical diffusivity.

6 Conclusions

In the present Report the numerical accuracy of the model for homogeneous conditions in a tidal flume situation has been investigated.

Before an evalution of the test results is given, it should be stressed that neither the numerical accuracy investigated in this Report nor the physical sensitivity [3] alone gives a good impression of the reliability and the predictive capability of the model. Therefore, it is necessary to combine the results of [3] and the present Report to get a complete impression of the model.

As far as the numerical accuracy goes, the following conclusions can be drawn:

- The vertical step size Δz is fixed by the accuracy of the computation of the tide. The minimum number of steps in the vertical direction is $N_z = 12$, and $N_z = 24$ yields a good accuracy.
- The horizontal step size Δx is fixed by the numerical diffusivity in the computation of the concentration. A minimal number of steps in the horizontal direction is $N_x = 50$. The only way to weaken this restriction is to find another discretisation for the diffusion equation, with less numerical diffusivity, especially near the boundaries.
- The size of the time step for the computation of the tide is fixed by the stabiltiy [5] and for the computation of the concentration by the numerical diffusivity. The most economical way of computation will be to choose different time steps for the tide and the concentration.

REFERENCES

1 Delft Hydraulics Laboratory,
Computation of density currents in estuaties,
Report on Mathematical Investigation, R 897 - III, December 1976, in Dutch.

2 Delft Hydraulics Laboratory,
Computations of a fresh water disposal into the Eastern Scheldt estuary,
Report on Mathematical Investigation, W 332, April 1978.

3 Delft Hydraulics Laboratory,
Computation of density currents in estuaties,
Report on Mathematical Investigation, R 897 - V, April 1979.

4 Delft Hydraulics Laboratory,
Computation of density currents in estuaties,
Report on Mathematical Investigation, R 897 - I, March 1975, in Dutch.

5 PERRELS, P.A.J. and KARELSE, M.,
A two-dimensional numerical model for salt intrusion in estuaries,
Delft Hydraulics Laboratory, Publication No. 177, November 1977.

no	N_x	Δx m	N_z	Δz m	N_t	τ s	ε_x $m^{\frac{1}{2}}s^{-1}$	D_x $m^{\frac{1}{2}}s^{-1}$	c $m^{\frac{1}{2}}s^{-1}$	cpu(cyber) 175 s
II 5	20	5.0325	20	.0108	600	.93125	.37	–	19.2	19.478
II 8	20	5.0325	20	.0108	600	.93125	.37	–	19.2	19.902
IV 1	20	5.0325	20	.0108	600	.93125	.37	–	29.4	20.244
IV 2	20	5.0325	20	.0108	600	.93125	.37	–	29.4	19.780
IV29	20	5.0325	20	.0108	600	.93125	.37	–	29.4	20.421
IV31	20	5.0325	20	.0108	600	.93125	.001	–	29.4	19.025
IV34	20	5.0325	6	.036	100	.93125	.37	–	29.4	1.490
IV35	20	5.0325	12	.018	100	.93125	.37	–	29.4	2.442
IV36	20	5.0325	24	.009	100	.93125	.37	–	29.4	4.361
RB16	13	7.46	12	.018	1200	1.8625	.37	.005	22.2/24.	17.371
RB17	13	7.46	12	.018	2400	.93125	.37	.005	22.2/24.	33.798
RB18	26	3.73	12	.018	2400	.93125	.37	.005	22.2/24.	62.501
RB49	13	7.46	12	.018	1200	1.8625	.37	.005	22.2/24.	17.542
RB21	13	7.46	6	.036	1200	1.8625	.37	.005	22.2/24.	11.062
RB22	13	7.46	24	.009	1200	1.8625	.37	.005	22.2/24.	31.527
RB24	13	7.46	12	.018	4800	.465625	.37	.005	22.2/24.	67.903
RB25	52	1.865	12	.018	2400	.93125	.37	.005	22.2/24.	125.359

Table I: List of Computations and Variations of Parameters

position / number	0.0 m	7.46 m	14.92 m	22.38 m	29.84 m	37.40 m	44.76 m	L_i* m
RB16	.9815	.7920	.5446	.2986	.1104	.0235	.0000	39.3
RB17	.9832	.8006	.5550	.3091	.1169	.0272	.0000	39.6
RB18	.9855	.7897	.5775	.3227	.0916	.0074	.0000	38.1
RB19	.9816	.7925	.5451	.2989	.1099	.0233	.0000	39.3
RB21	.9796	.7755	.5181	.2786	.0996	.0214	.0000	39.4
RB22	.9819	.7966	.5548	.3075	.1163	.0247	.0000	39.3
RB24	.9836	.8034	.5586	.3130	.1203	.0289	.0000	39.7
RB25	.9918	.7858	.5716	.3227	.0856	.0039	.0000	37.6

Table II: Depth-averaged Concentrations at Maximal Intrusion and the Intrusion Length

* The maximal intrusion length L_i is found from a linear extrapolation of the concentrations in x = 29.84 m and x = 37.30 m.

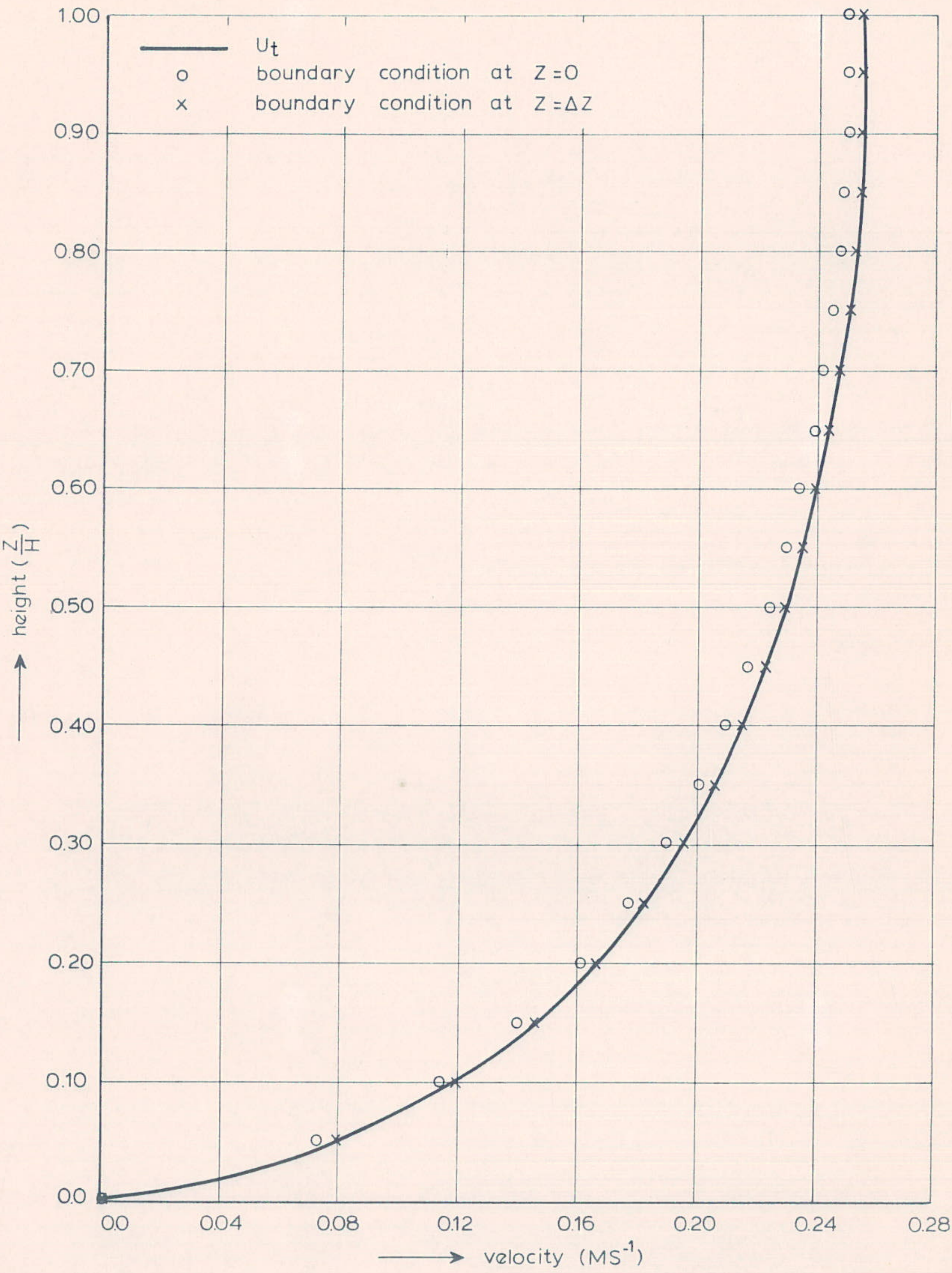

VELOCITY PROFILES FOR C = 19.2

DELFT HYDRAULICS LABORATORY

R 897 - IV

FIG. 1

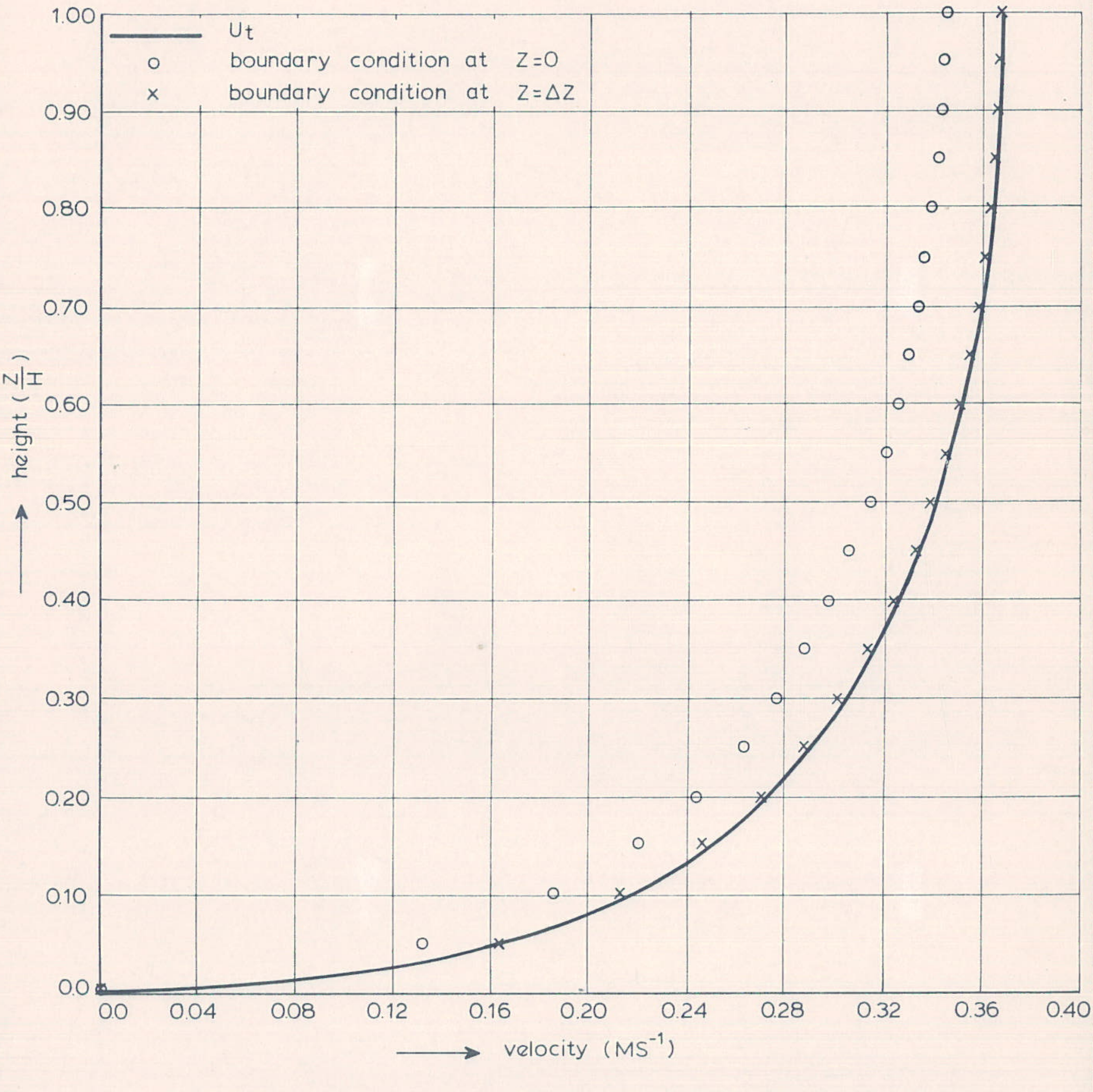

VELOCITY PROFILES FOR C = 29.4

DELFT HYDRAULICS LABORATORY | R 897 - IV | FIG. 2

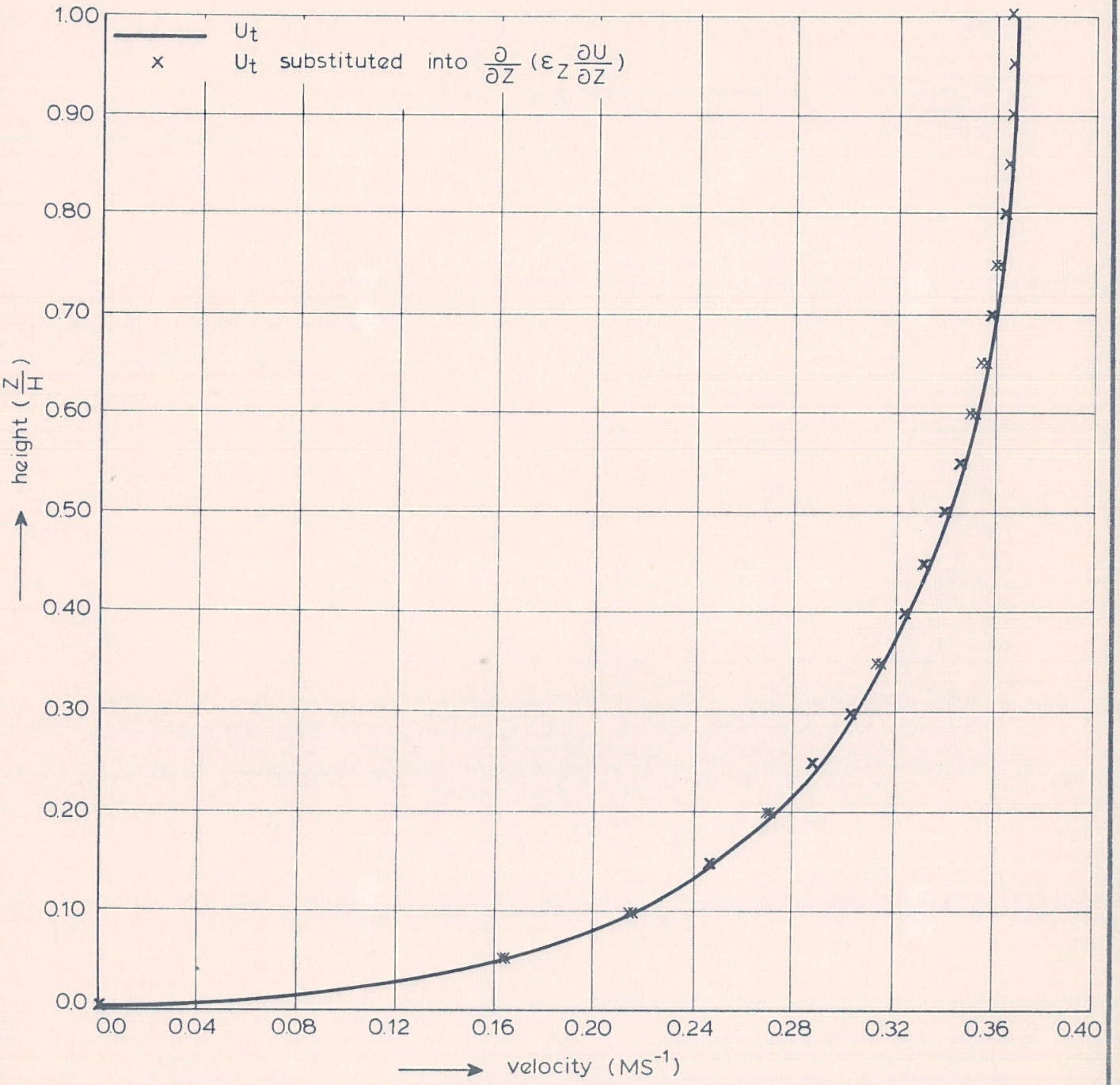

VELOCITY PROFILES FOR C = 29.4		
DELFT HYDRAULICS LABORATORY	R 897 - IV	FIG. 3

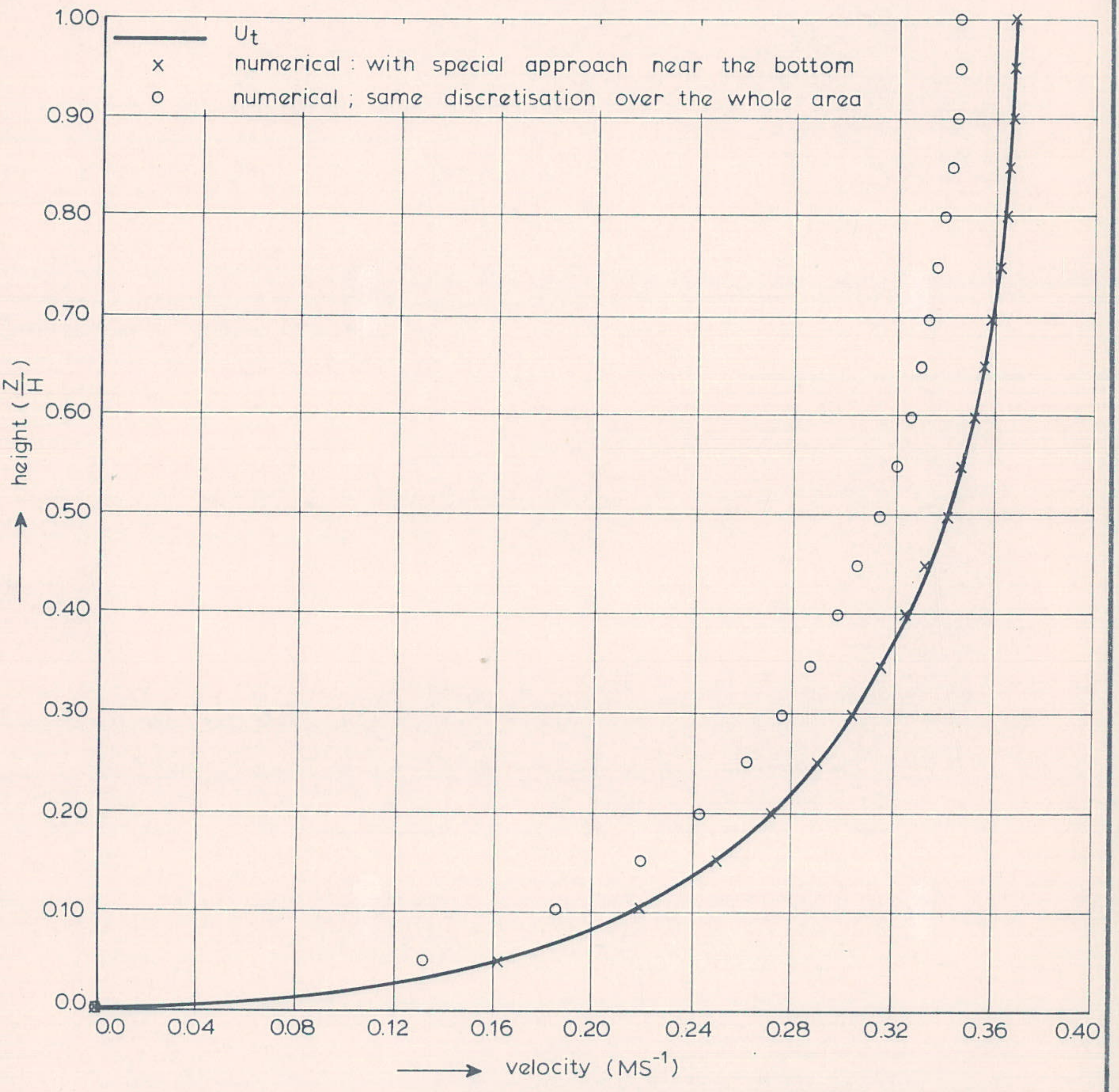

VELOCITY PROFILES FOR C = 29.4

DELFT HYDRAULICS LABORATORY	R 897 - IV
	FIG. 4

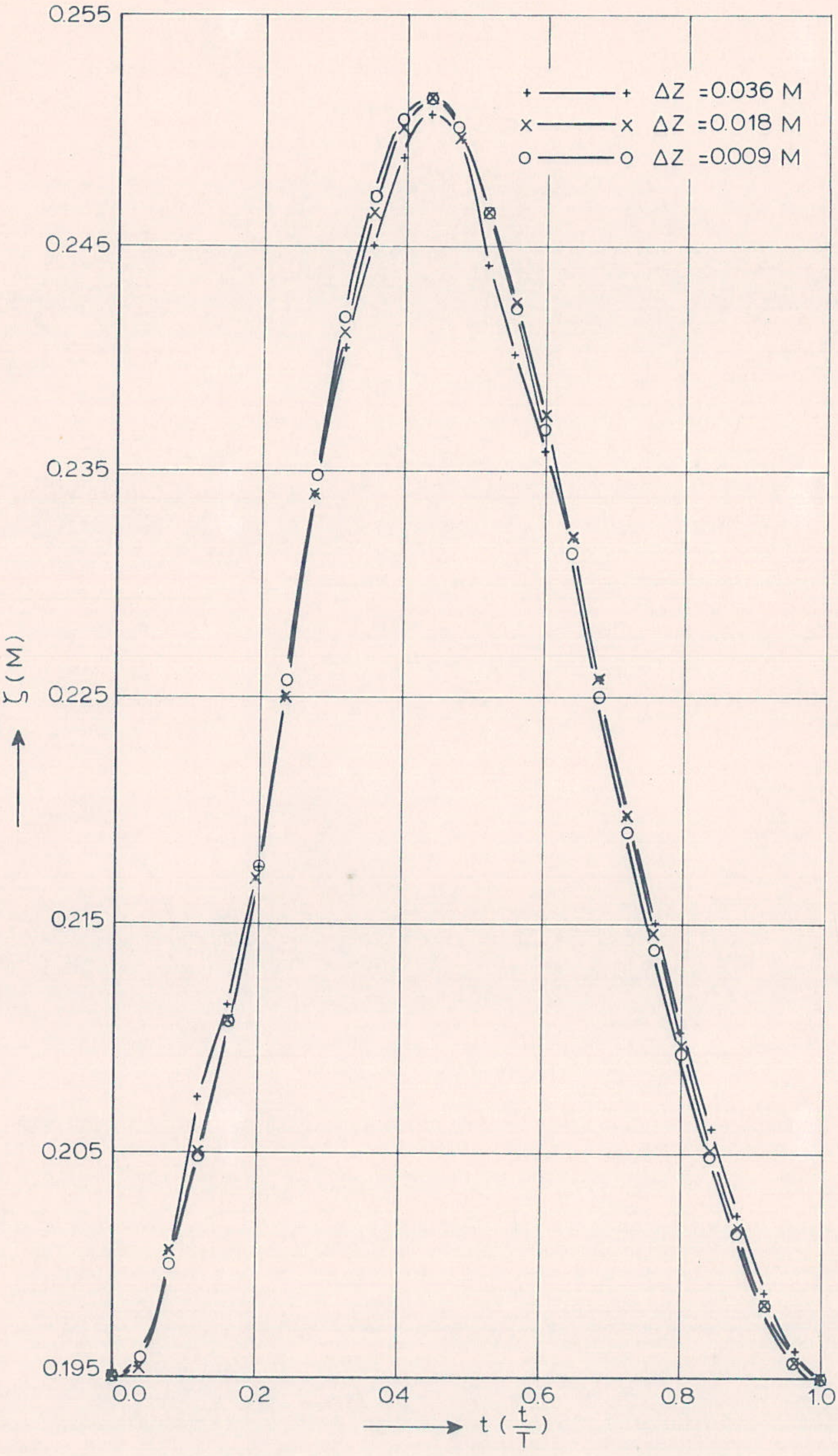

INFLUENCE OF THE VERTICAL STEPSIZE : ΔZ
POSITION OF THE FREE SURFACE AT : X = L

DELFT HYDRAULICS LABORATORY

R 897-IV

FIG. 5

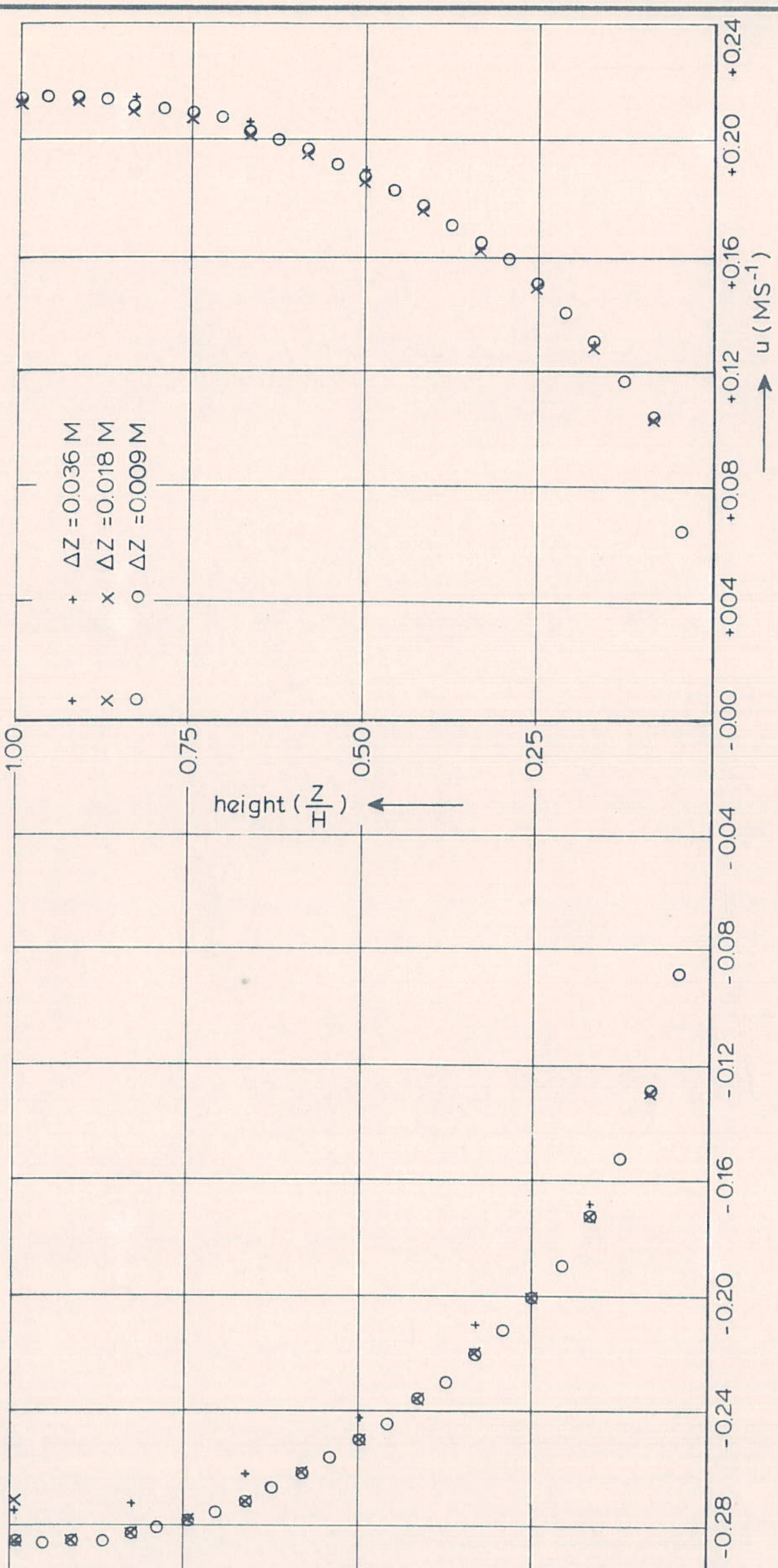

INFLUENCE OF THE VERTICAL STEPSIZE : ΔZ
VELOCITY PROFILES AT M.F.V. AND M.E.V.
AT : X = 0.0 M

DELFT HYDRAULICS LABORATORY | R 897 - IV | FIG. 6

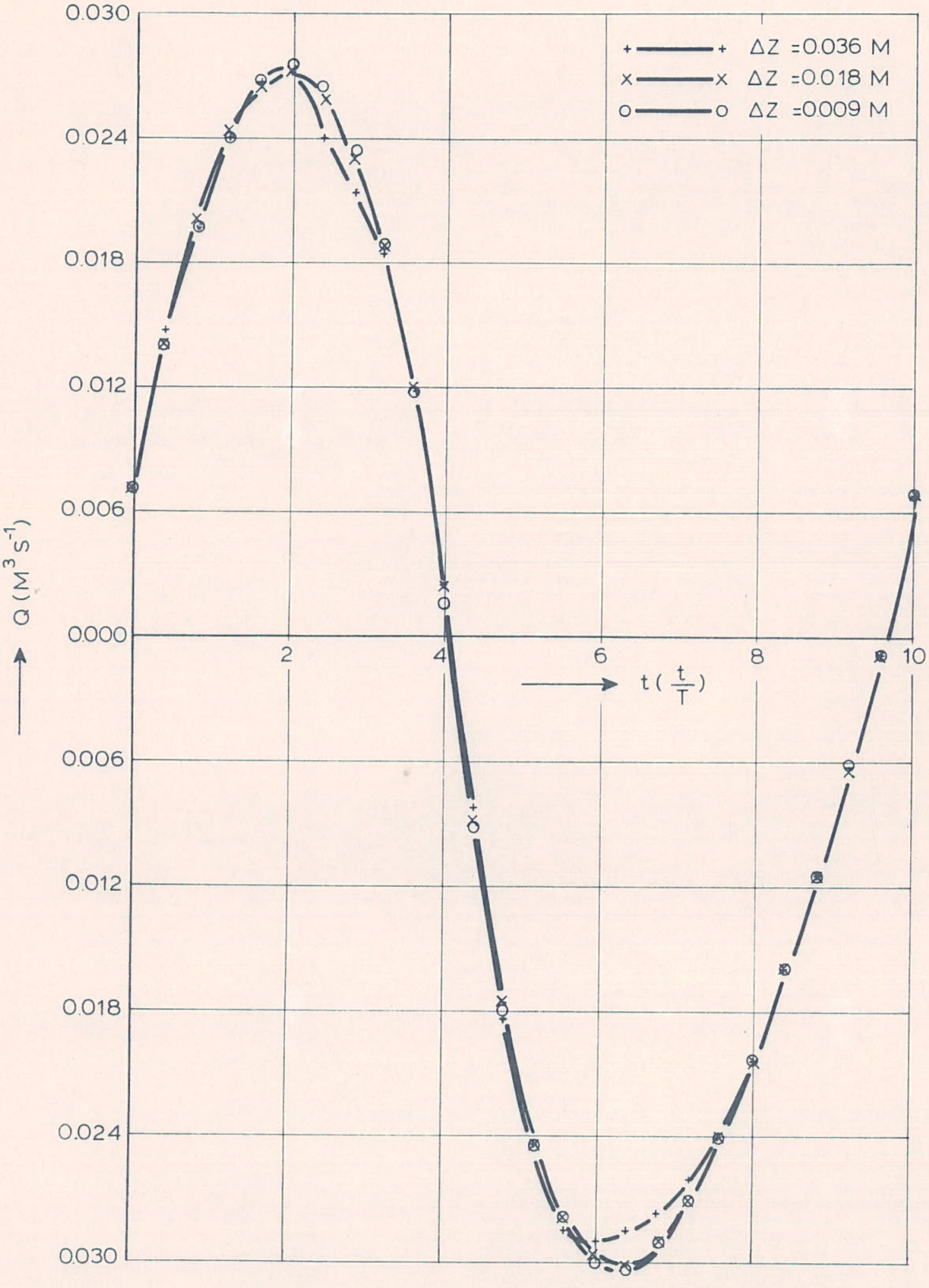

INFLUENCE OF THE VERTICAL STEPSIZE : ΔZ
DISCHARGES AT x = 0.0 M

DELFT HYDRAULICS LABORATORY

R 897 - IV

FIG. 7

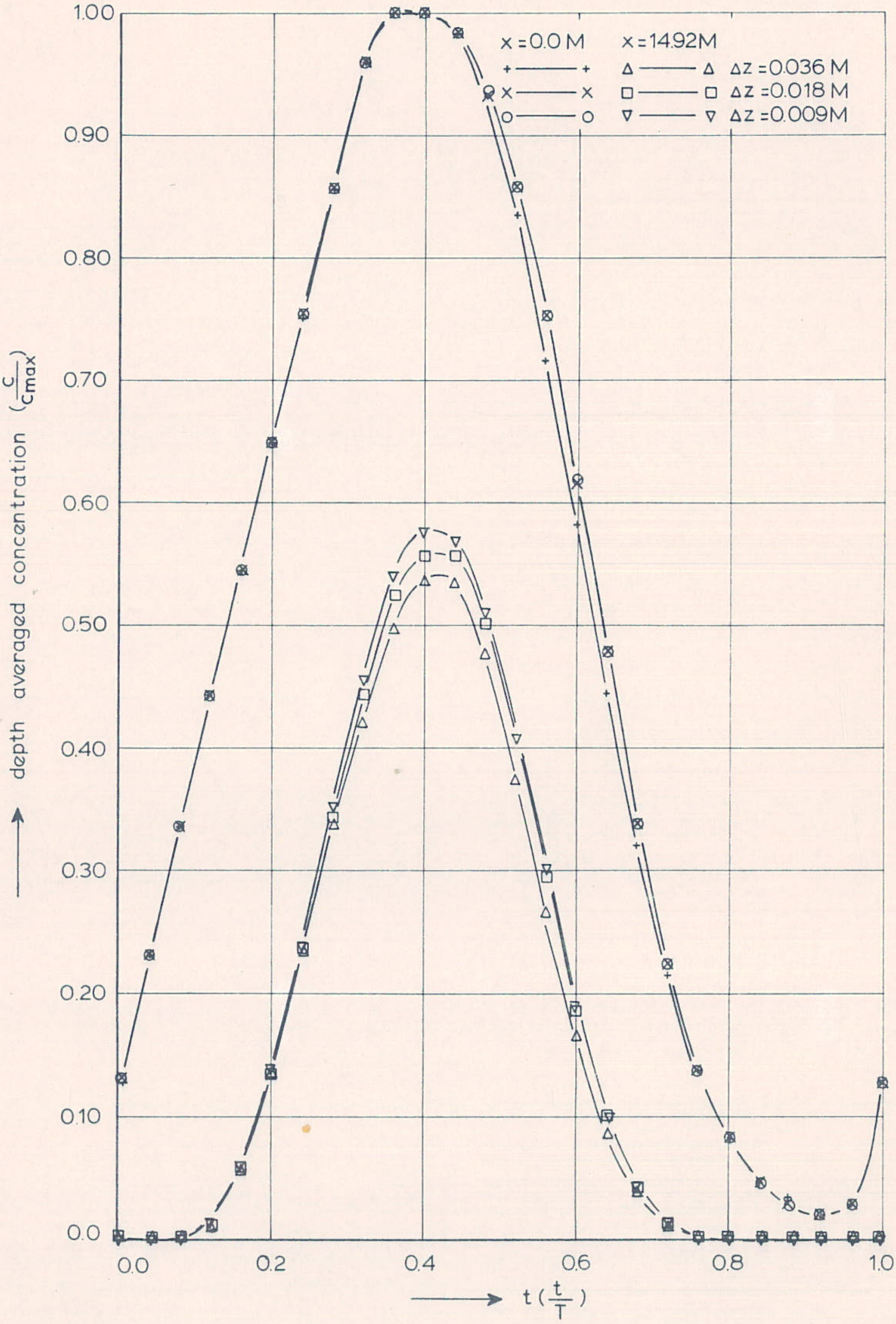

INFLUENCE OF THE VERTICAL STEPSIZE : Δz
CONCENTRATIONS AT x=0.0 M AND x=14.92 M

DELFT HYDRAULICS LABORATORY | R 897-IV | FIG. 8

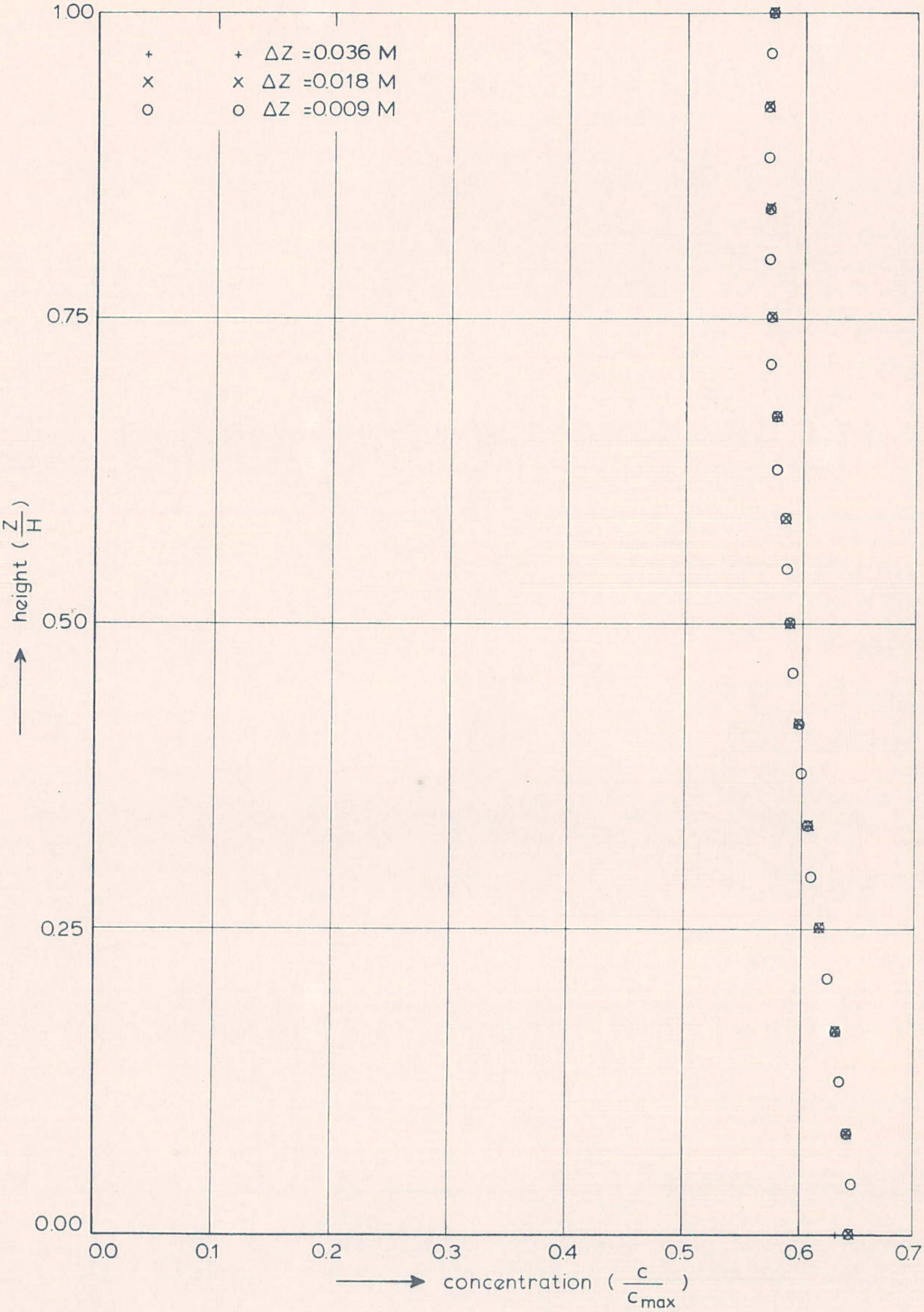

INFLUENCE OF THE VERTICAL STEPSIZE : ΔZ
CONCENTRATIONS AT x = 0.0 M AT M.F.V.

DELFT HYDRAULICS LABORATORY | R 897 - IV | FIG. 9

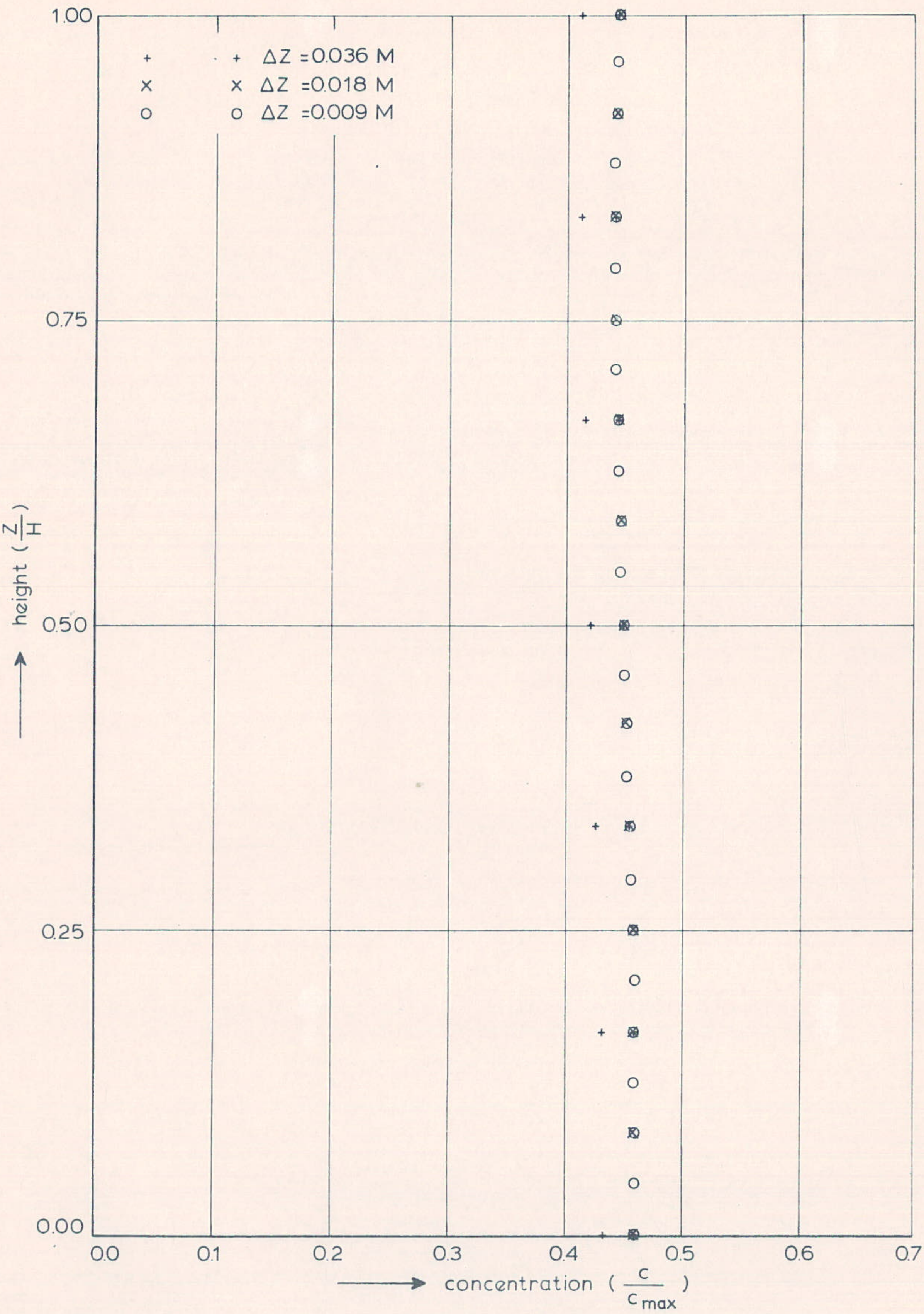

INFLUENCE OF THE VERTICAL STEPSIZE : ΔZ
CONCENTRATIONS AT x = 0.0 M AT M.E-V.

DELFT HYDRAULICS LABORATORY | R 897 - IV | FIG. 10

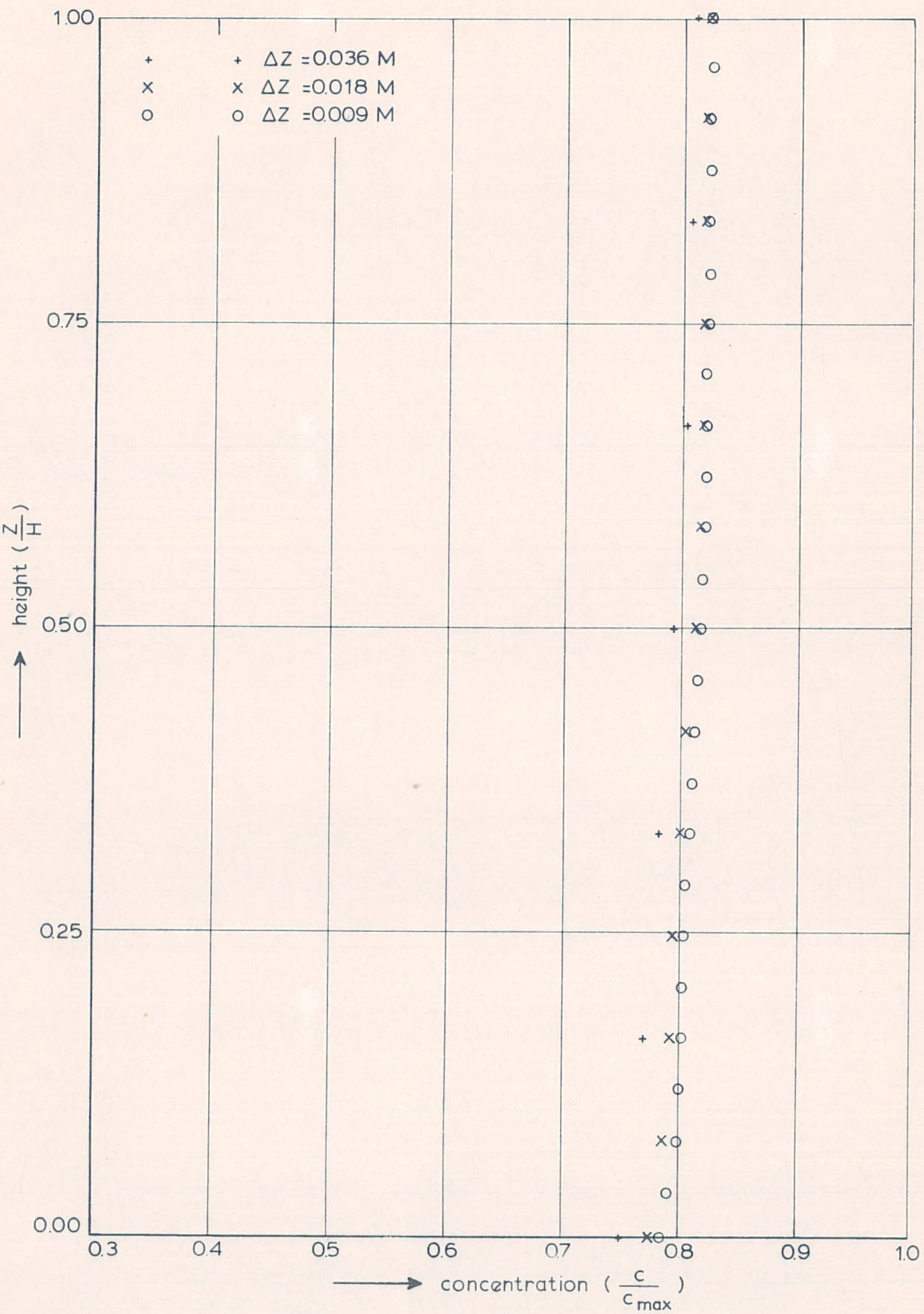

INFLUENCE OF THE VERTICAL STEPSIZE : ΔZ
MAXIMAL CONCENTRATIONS AT X = 7.46 M

DELFT HYDRAULICS LABORATORY	R 897 - IV	FIG. 11

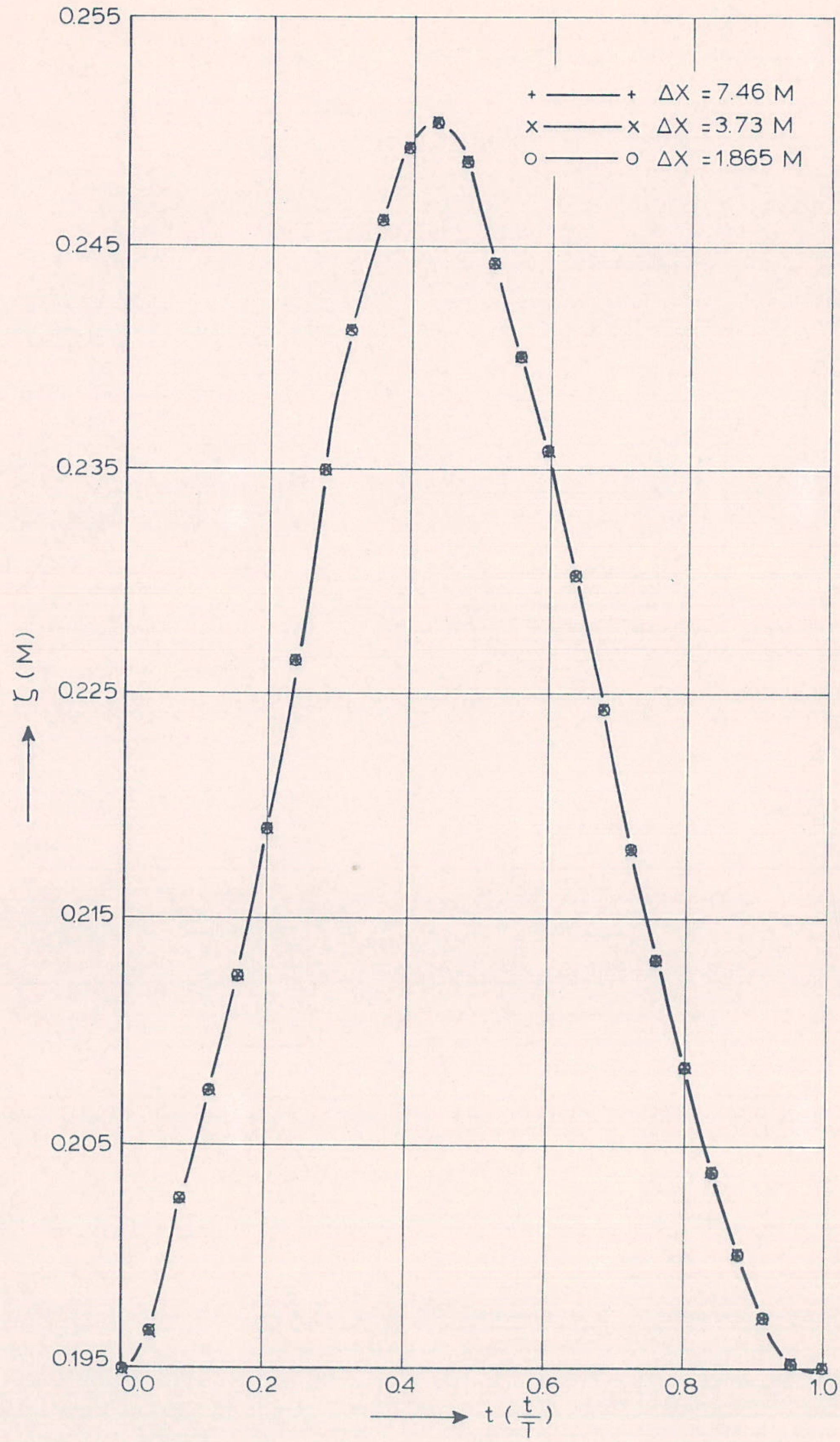

INFLUENCE OF THE HORIZONTAL STEPSIZE : ΔX
POSITION OF THE FREE SURFACE AT : X = L

DELFT HYDRAULICS LABORATORY | R 897-IV | FIG. 12

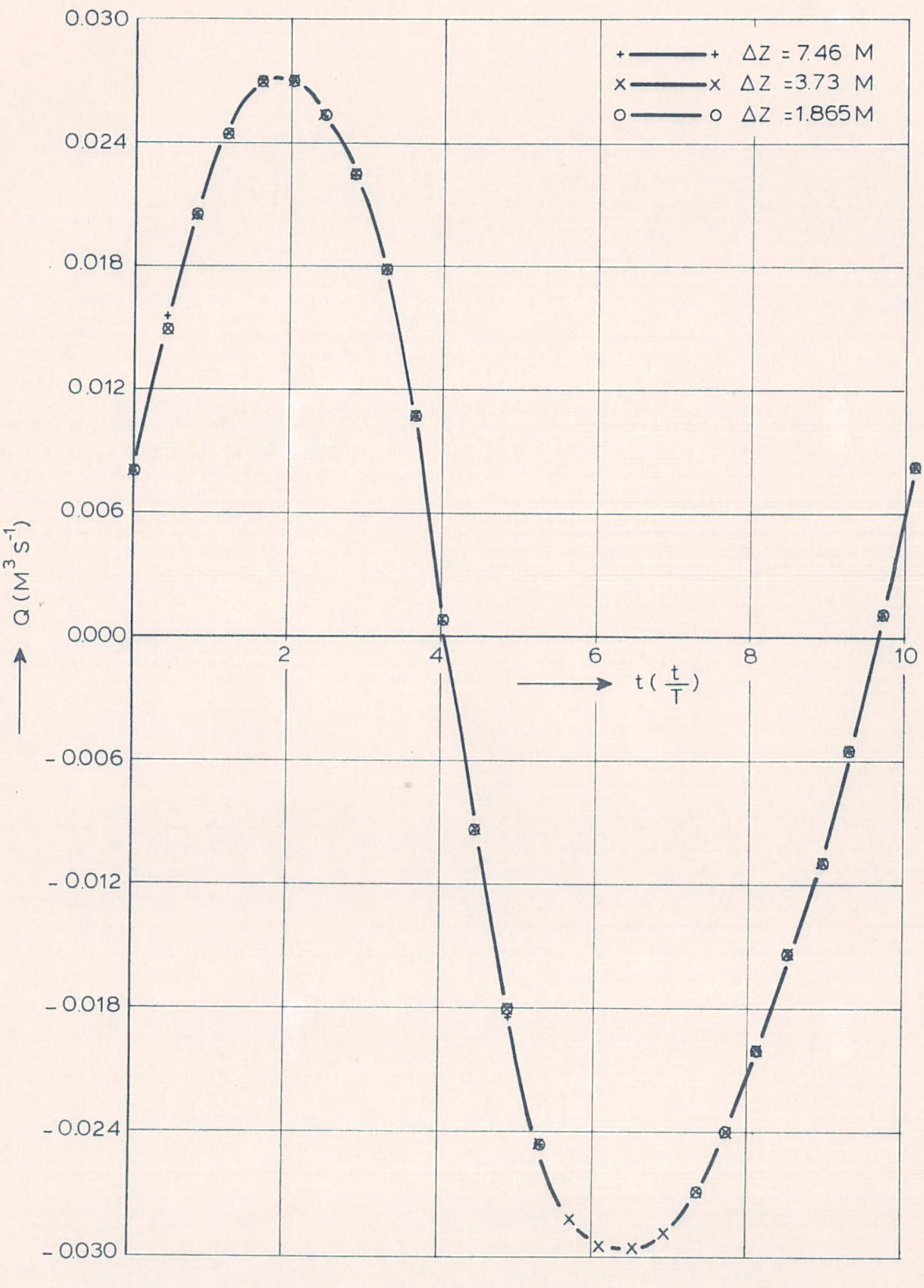

INFLUENCE OF THE HORIZONTAL STEPSIZE : ΔZ
DISCHARGES AT x = 0.0 M

DELFT HYDRAULICS LABORATORY

R 897 - IV | FIG. 13

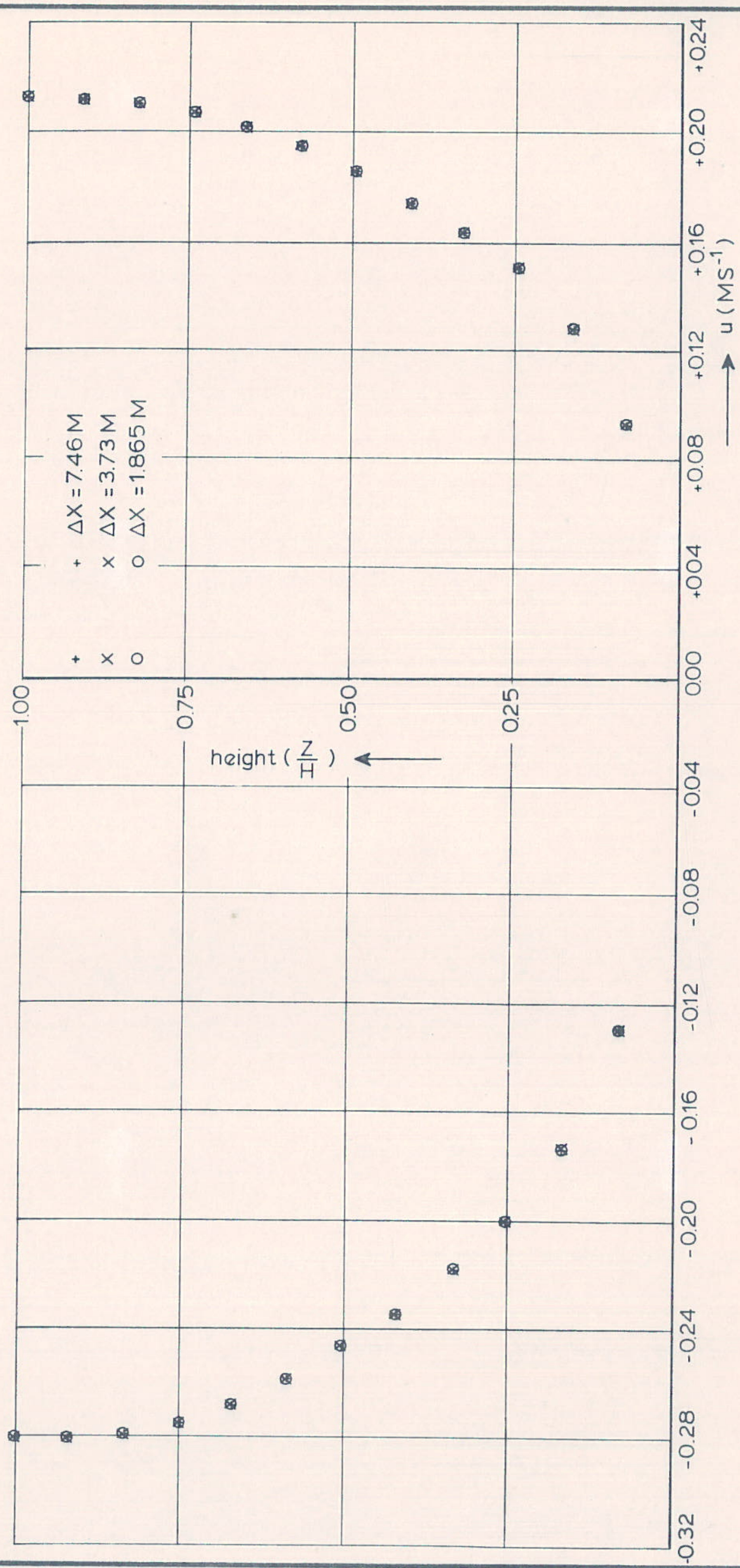

INFLUENCE OF THE HORIZONTAL STEPSIZE: ΔX
VELOCITY PROFILES AT M.F.V. AND M.E.V.
AT: X = 0.0 M

DELFT HYDRAULICS LABORATORY	R 897 - IV	FIG. 14

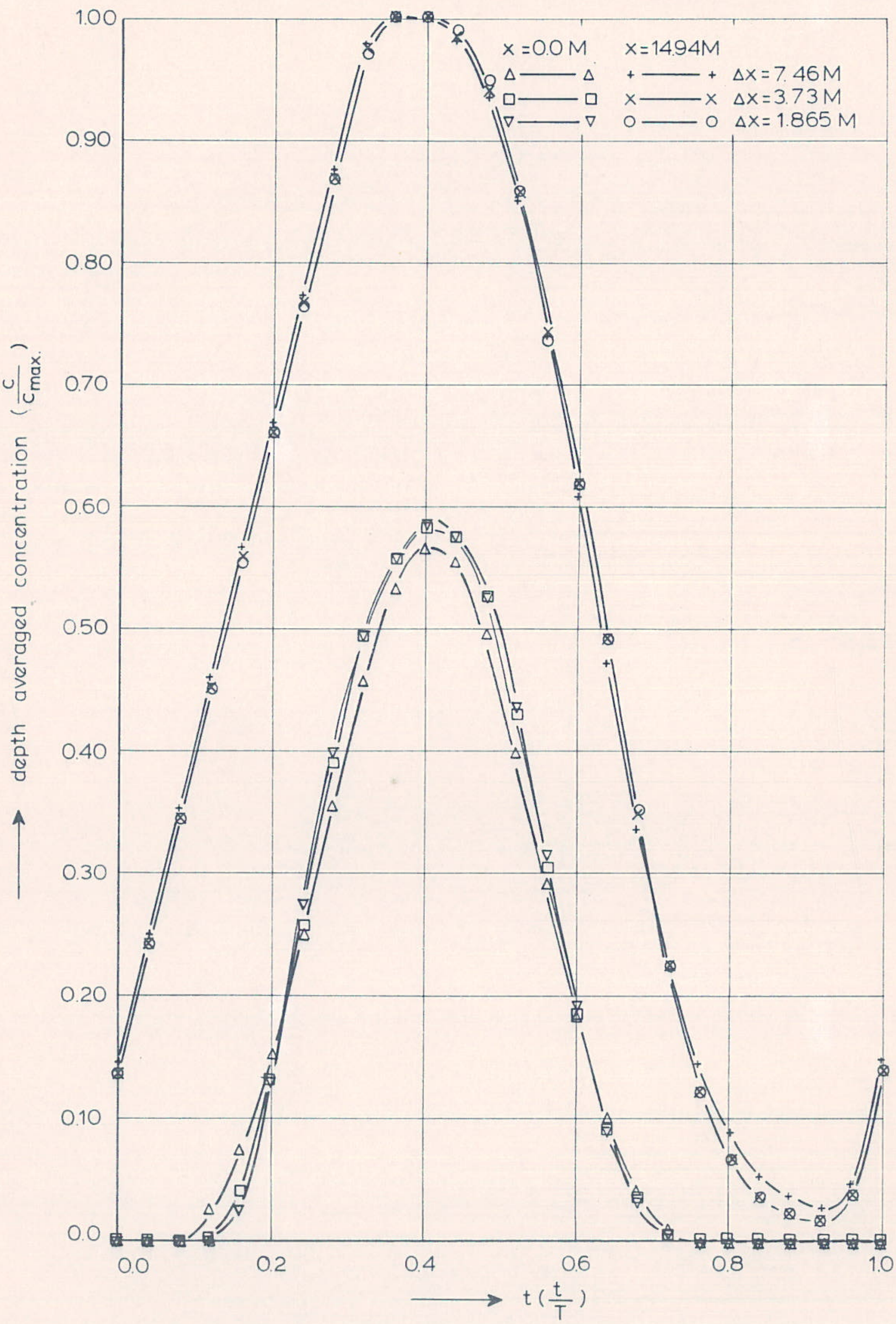

INFLUENCE OF THE HORIZONTAL STEPSIZE : Δx
CONCENTRATIONS AT x = 0.0 M AND x = 14.92 M

DELFT HYDRAULICS LABORATORY	R 897 - IV	FIG. 15

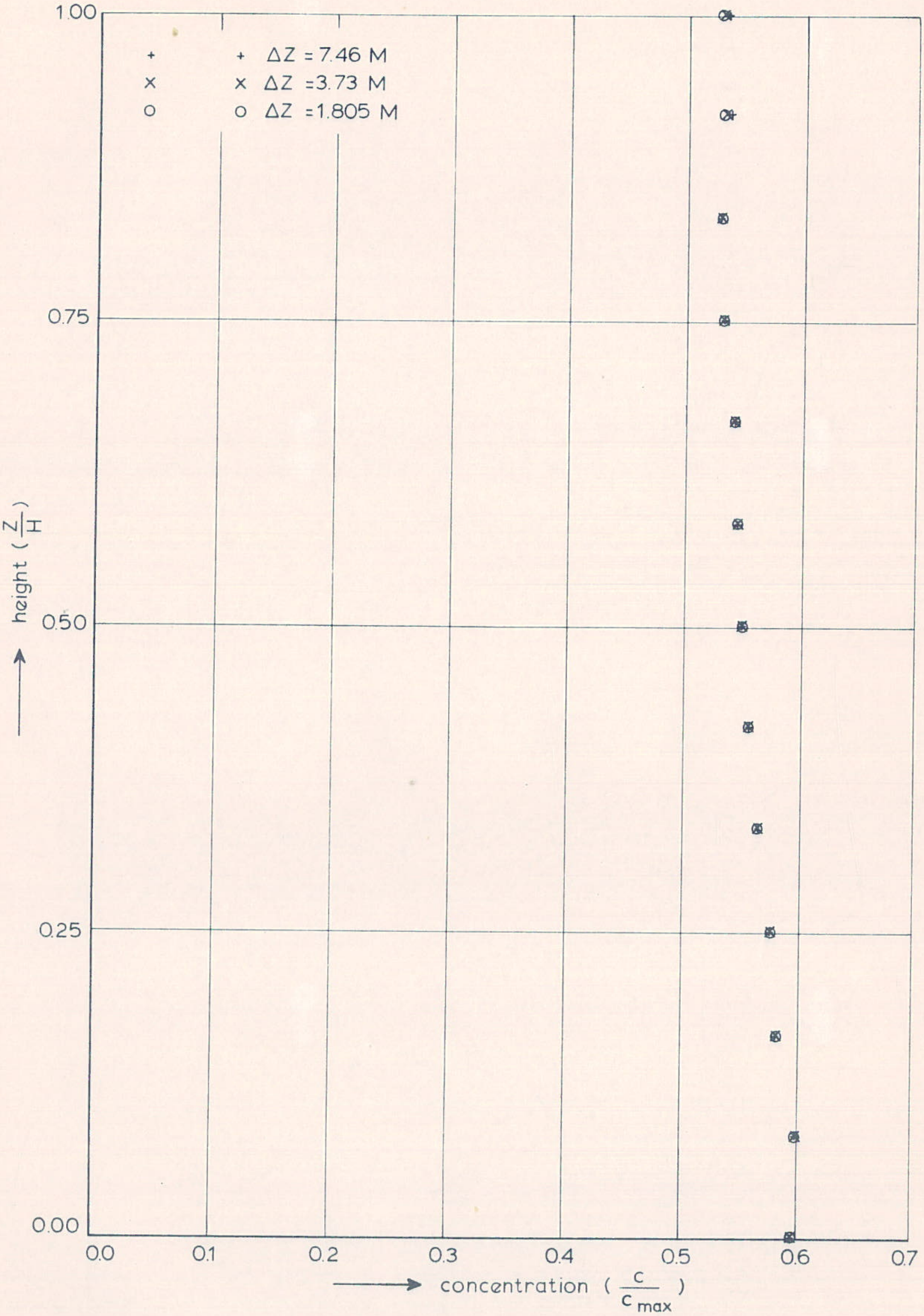

INFLUENCE OF THE HORIZONTAL STEPSIZE : ΔX CONCENTRATIONS AT X = 0.0 M AT M.F.V.		
DELFT HYDRAULICS LABORATORY	R 897 - IV	FIG. 16

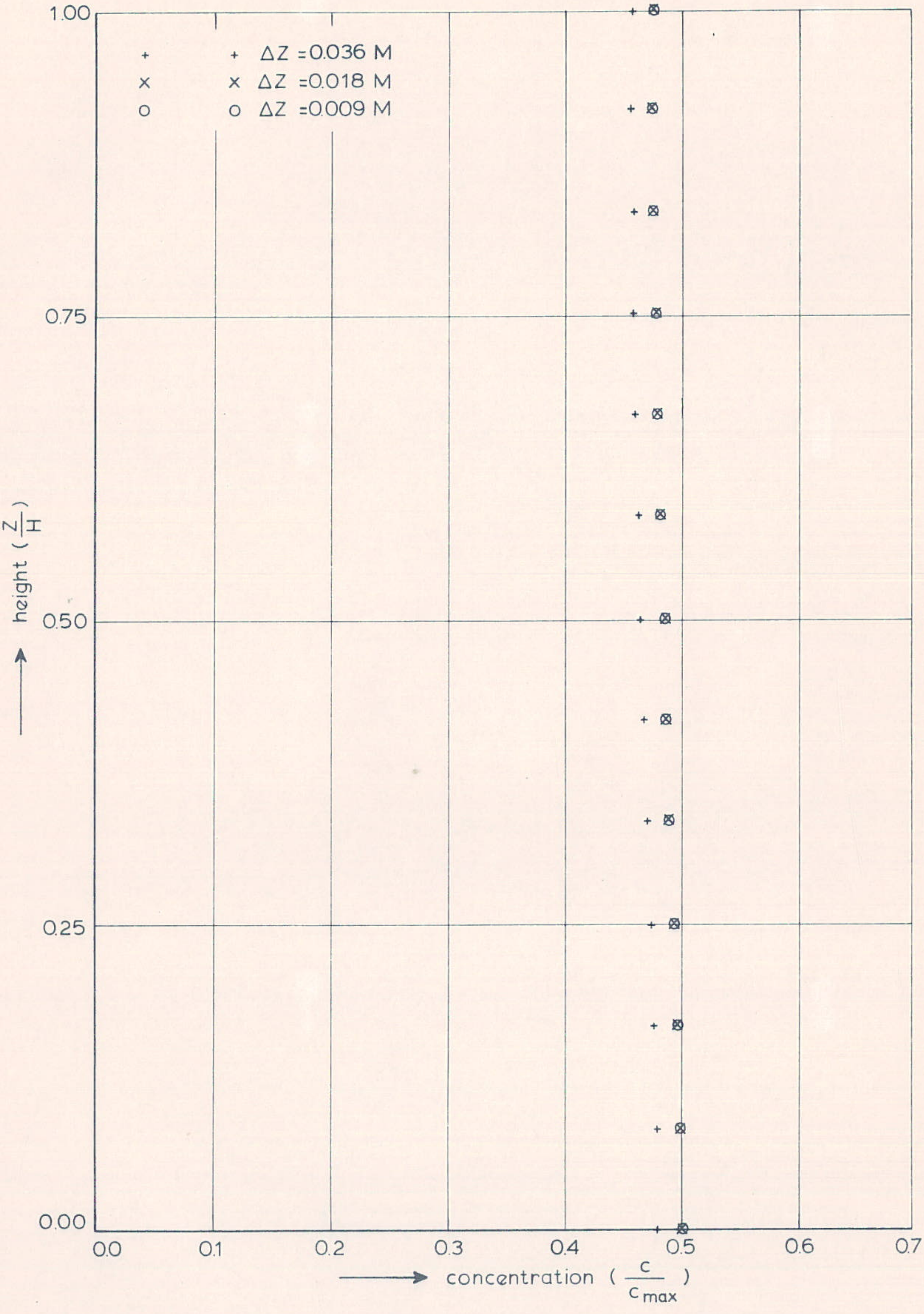

INFLUENCE OF THE HORIZONTAL STEPSIZE : ΔX
CONCENTRATIONS AT X = 0.0M AT M.E.V.

DELFT HYDRAULICS LABORATORY | R 897 - IV | FIG. 17

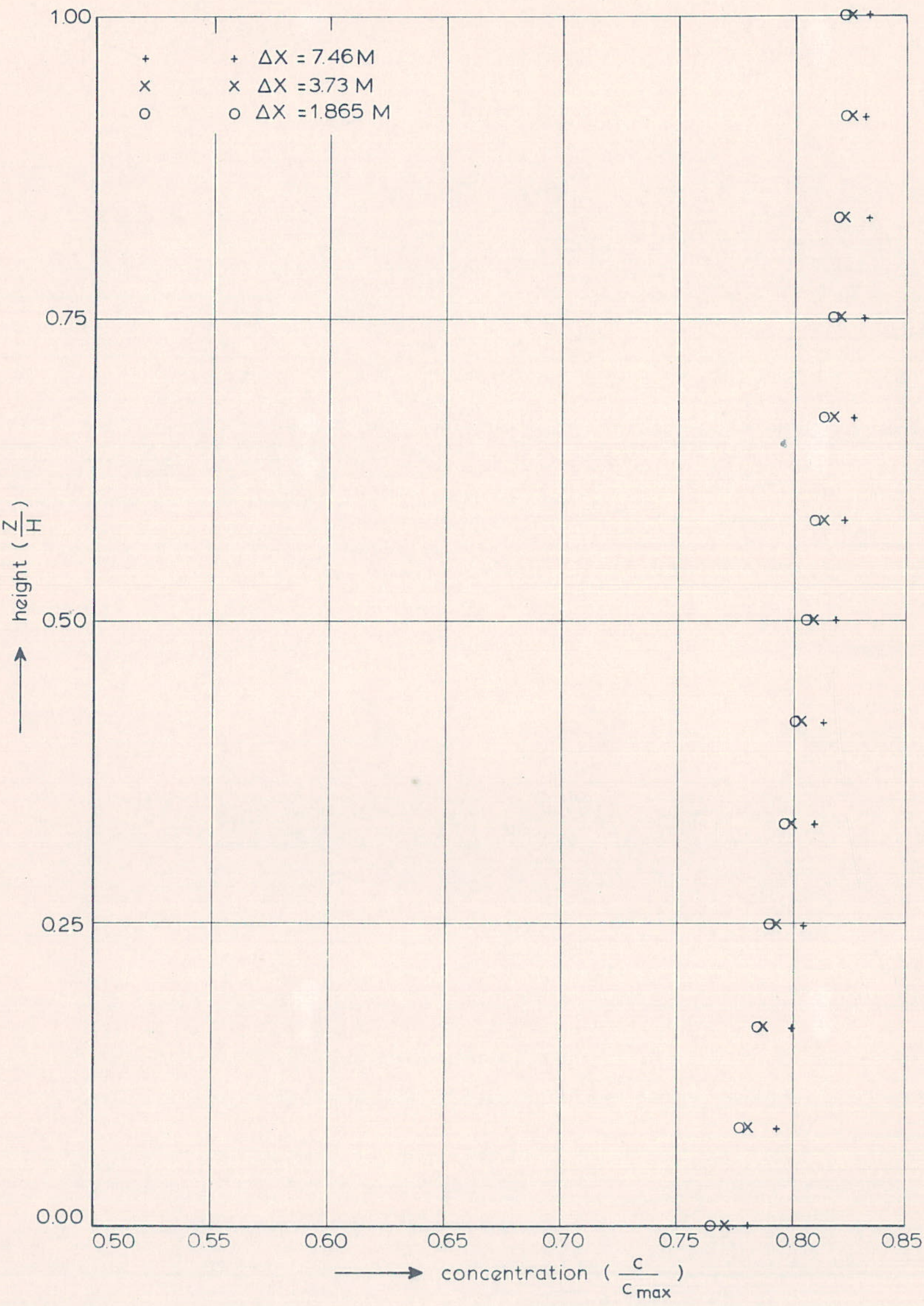

INFLUENCE OF THE HORIZONTAL STEPSIZE : ΔX

MAXIMAL CONCENTRATION AT X = 7.46 M

DELFT HYDRAULICS LABORATORY

R 897 - IV

FIG. 18

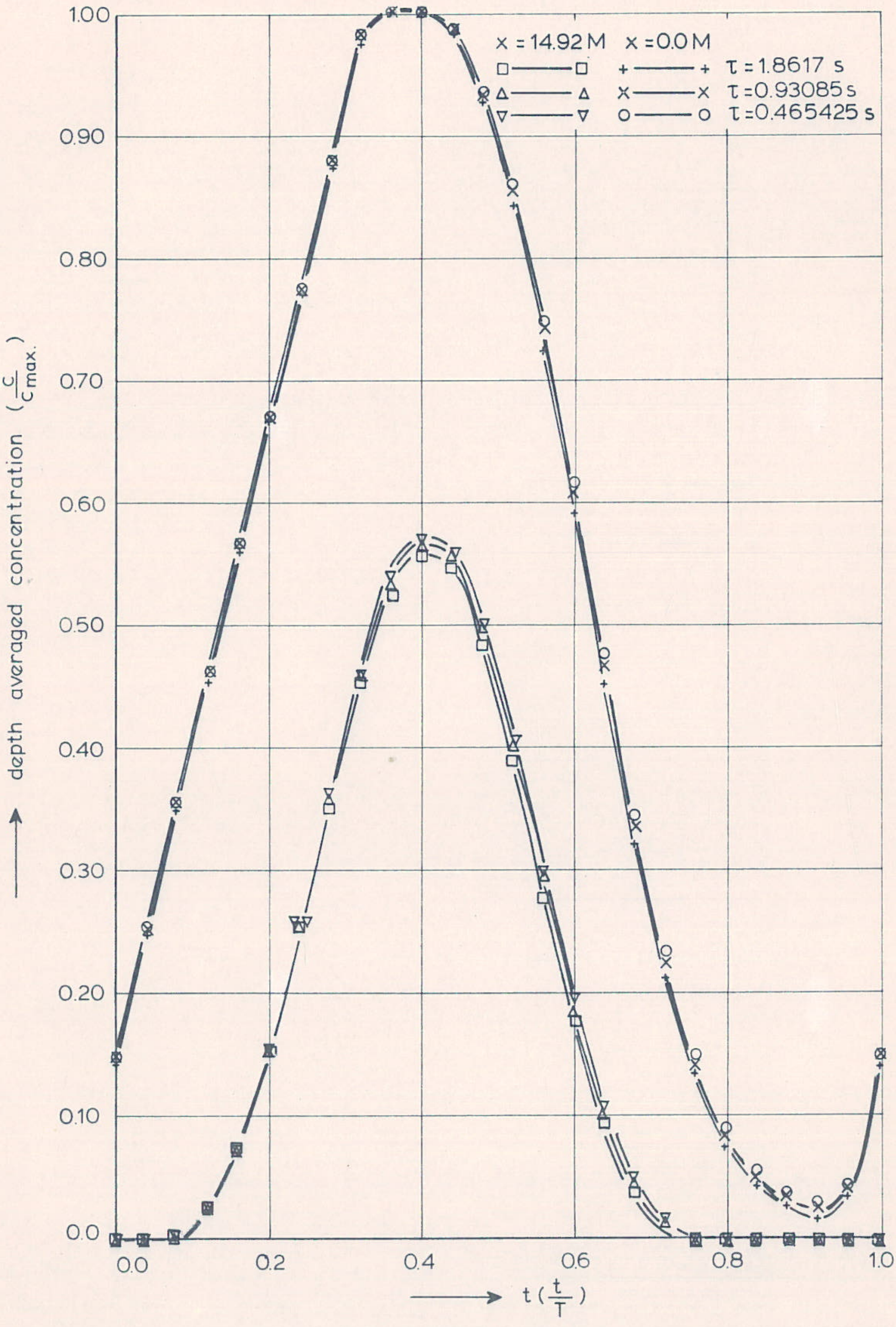

INFLUENCE OF THE TIMESTEP : τ
CONCENTRATIONS AT x=0.0 M AND x̃=14.92 M

DELFT HYDRAULICS LABORATORY	R 897 - IV	FIG. 19

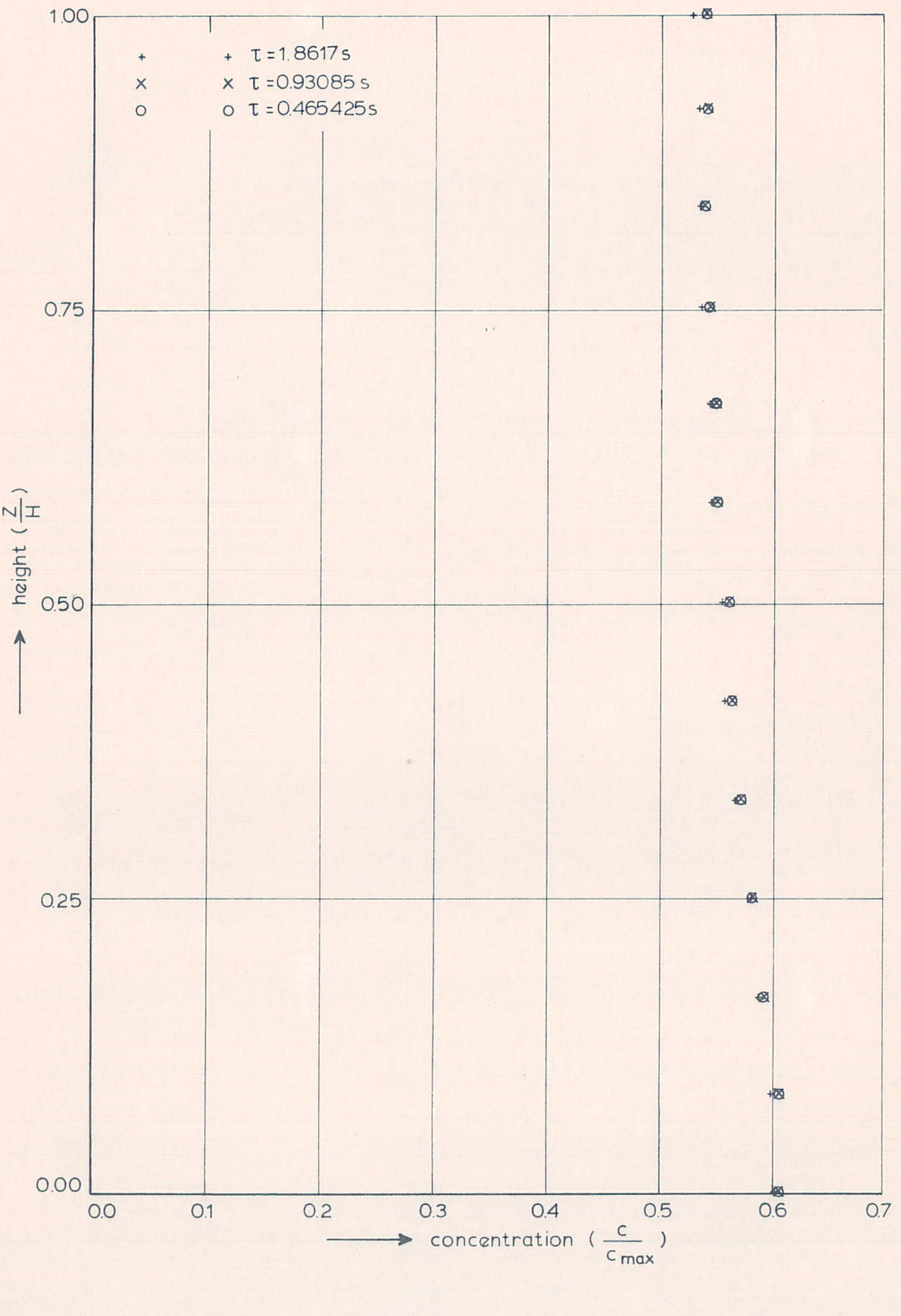

INFLUENCE OF THE TIMESTEP : τ
CONCENTRATIONS AT X = 0.0 M AT M.F.V.

DELFT HYDRAULICS LABORATORY | R 897 - IV | FIG. 20

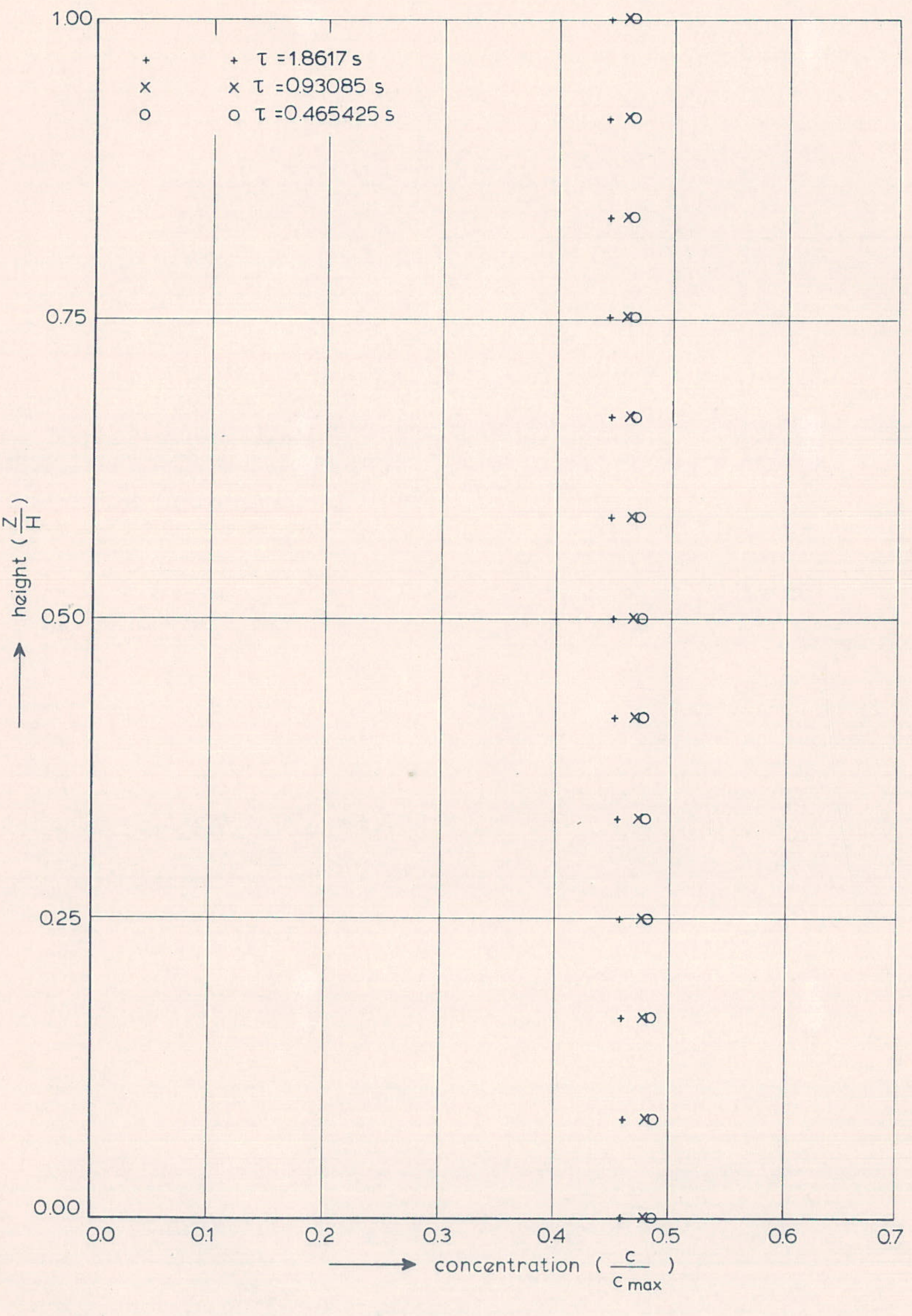

INFLUENCE OF THE TIMESTEP : τ
CONCENTRATIONS AT X = 0.0 M AT M.E.V.

DELFT HYDRAULICS LABORATORY | R 897 - IV | FIG. 21

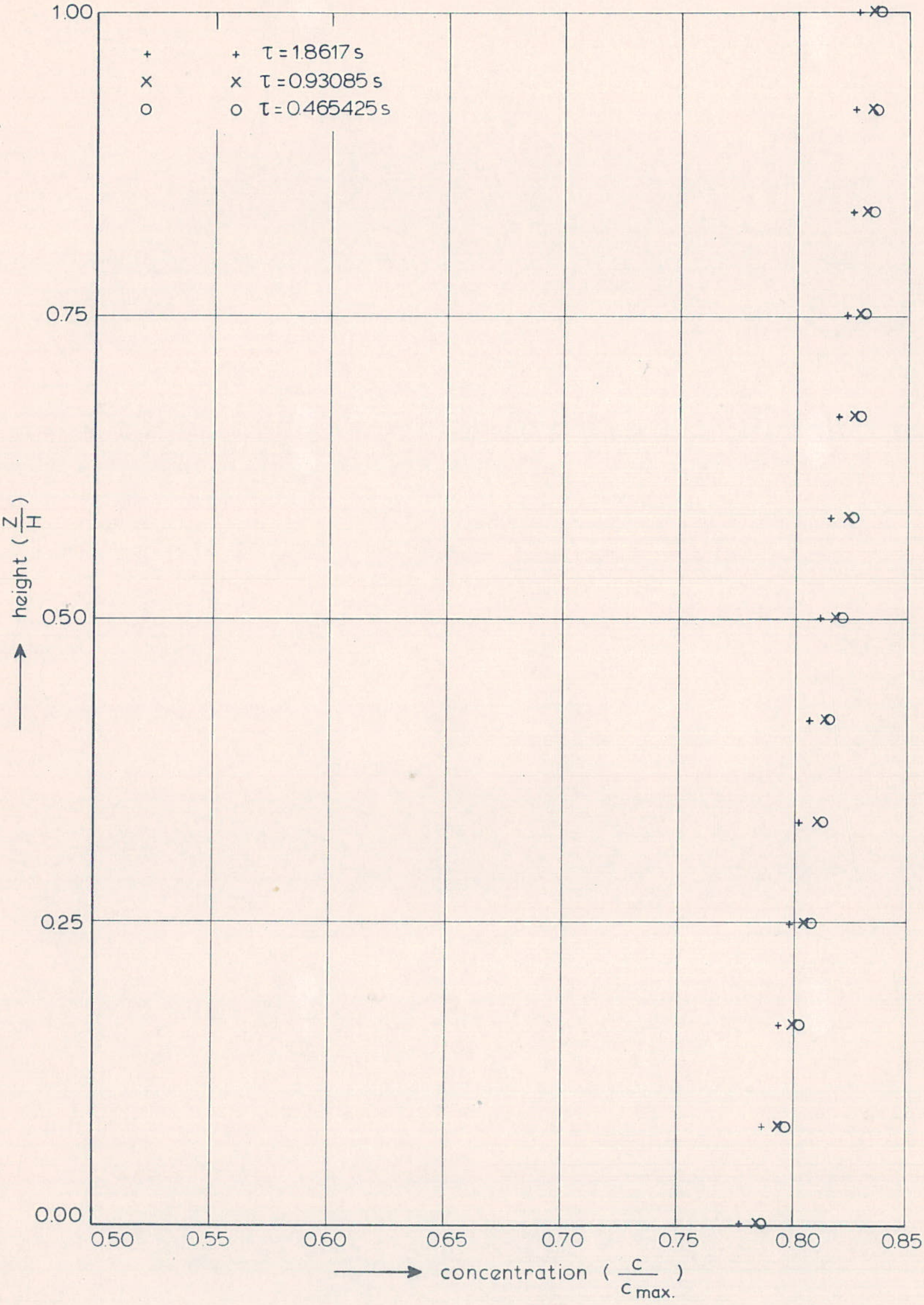

INFLUENCE OF THE TIMESTEP : τ
MAXIMAL CONCENTRATION AT X = 7.46 M

DELFT HYDRAULICS LABORATORY

R 897 - IV

FIG. 22

APPENDIX I: Fixing the Singular Behaviour of u near the Bottom

For steady uniform turbulent flow it can be shown that the velocity behaves logarithmically near the fixed bottom.

For unsteady non-uniform flow no closed analytical solution can be given. Estimating, however, the order of magnitude of several terms of the equation for conservation of momentum indicates that near the bottom u behaves logarithmically

$$\text{Suppose : } u \sim \ln\left(\frac{z + z_0}{z_0}\right) \qquad (1a)$$

Then substitution of (1a) into the continuity equation yields:

$$w \sim z - z \ln\left(\frac{z + z_0}{z_0}\right) \qquad (2a)$$

Substituting (1a) and (2a) into the equation for conservation of momentum:

$$\frac{\partial u}{\partial t} + \frac{\partial u^2}{\partial x} + \frac{\partial uw}{\partial z} - \varepsilon_x \frac{\partial^2 u}{\partial^2} - \frac{\partial}{\partial z}\left(\varepsilon_z \frac{\partial u}{\partial z}\right) = -\frac{1}{\rho}\frac{\partial p}{\partial x} \qquad (3a)$$

yields the following orders of magnitude for the successive terms of (3a)

$$\ln\left(\frac{z + z_0}{z_0}\right),\ \left\{\ln\left(\frac{z + z_0}{z_0}\right)\right\}^2,\ \ln\left(\frac{z + z_0}{z_0}\right) + \frac{z}{z_o},\ \ln\left(\frac{z + z_0}{z_0}\right),\quad O(1),\ O(1)$$

so near the bottom approximately the following equation holds:

$$\frac{\partial}{\partial z}\left(\varepsilon_z \frac{\partial u}{\partial z}\right) = \frac{1}{\rho}\frac{\partial p}{\partial x} \qquad (4a)$$

and if a mixing length approach is adopted for ε_z:

$$\varepsilon_z = \kappa^2 (z + z_0)^2 \left|\frac{\partial u}{\partial z}\right| \qquad (5a)$$

(4a) will yield:

$$u \sim \ln \frac{z + z_0}{z_0}$$

which is in agreement with (1a)

APPENDIX II: Derivation of the Pressure Distribution for a Given Velocity Profile

The following expression for the horizontal velocity is adopted:

$$u = u_0 \sin(\omega t + kx) \{\ln (\frac{z + z_0}{z_0}) - \frac{z^2}{2 H^2}\}, \tag{6a}$$

in which the sine function reflects the tidal influence, the logarithm reflects the behaviour near the bottom and herein $\frac{z^2}{2 H^2}$ is included to provide a simple boundary condition at the free surface.

Substituting (6a) into the continuity equation:

$$\frac{\partial u}{\partial x} + \frac{\partial w}{\partial z} = 0 \tag{7a}$$

yields:

$$\frac{\partial w}{\partial z} + u_0 k \cos (\omega t + kx) \{\ln (\frac{z + z_0}{z_0}) - \frac{z^2}{2 H^2}\} = 0 \tag{8a}$$

Integrating (8a) and substituting the boundary condition:

$$w = 0 \quad \text{at} \quad z = 0 \tag{9a}$$

yields:

$$w = - u_0 k \cos (\omega t + kx) \{(z + z_0) \ln (\frac{z + z_0}{z_0}) - z - \frac{z^3}{6 N^2}\} \tag{10a}$$

If (7a) is substituted into the equation of conservation of momentum in the x-direction:

$$\frac{\partial u}{\partial t} + \frac{\partial u^2}{\partial x} + \frac{\partial uw}{\partial z} - \varepsilon_x \frac{\partial^2 u}{\partial x^2} - \frac{\partial}{\partial z} (\varepsilon_z \frac{\partial u}{\partial z}) = - \frac{1}{\rho} \frac{\partial p}{\partial x} \tag{3a}$$

reordering yields:

$$\frac{\partial p}{\partial x} = - \rho \{\frac{\partial u}{\partial t} + u \frac{\partial u}{\partial x} + w \frac{\partial u}{\partial z} - \varepsilon_x \frac{\partial^2 u}{\partial x^2} - \frac{\partial}{\partial z} (\varepsilon_z \frac{\partial u}{\partial z})\} \tag{11a}$$

Differentiating (6a) with respect to t yields:

$$\frac{\partial u}{\partial t} = u_0\ \omega \cos (\omega t + kx)\ \{\ln (\frac{z + z_0}{z_0}) - \frac{z^2}{2\ H^2}\} \tag{12a}$$

Differentiating (6a) with respect to x yields:

$$\frac{\partial u}{\partial x} = u_0\ k \cos (\omega t + kx)\ \{\ln (\frac{z + z_0}{z_0}) - \frac{z^2}{2\ H^2}\} \tag{13a}$$

Differentiating (6a) with respect to z yields:

$$\frac{\partial u}{\partial z} = u_0 \sin (\omega t + kx)\ \{\frac{1}{(z + z_0)} - \frac{z}{H^2}\} \tag{14a}$$

Differentiating (13a) with respect to x yields:

$$\frac{\partial^2 u}{\partial x^2} = -\ u_0\ k^2 \sin (\omega t + kx)\ \{\ln (\frac{z + z_0}{z_0}) - \frac{z^2}{2\ H^2}\}. \tag{15a}$$

For ε_z a mixing length approach is used:

$$\varepsilon_z = \kappa^2\ (z + z_0)^2\ |\frac{\partial u}{\partial z}|. \tag{16a}$$

Substituting (14a) into (16a) yields:

$$\varepsilon_z = u_0\ \kappa^2\ |\sin (\omega t + kx)|\ \{(z + z_0) - \frac{z(z + z_0)^2}{H^2}\} \tag{17a}$$

Multiplying (14a) by (17a) and differentiating with respect to z yields:

$$\frac{\partial}{\partial z}\ (\varepsilon_z \frac{\partial u}{\partial z}) = u_0{}^2\ \kappa^2 \sin (\omega t + kx)\ |\sin (\omega t + kx)|$$

$$\{- \frac{2\ z_0}{H^2} - \frac{4z}{H^2} + \frac{2\ z(z + z_0)\ (2\ z + z_0)}{H^4}\} \tag{18a}$$

Substituting (6a), (10a), (12a), (13a), (14a), (15a) and (18a) into (11a) yields:

$$\frac{\partial p}{\partial x} = -\ \rho \Bigg[u_0\ \omega \cos(\omega t + kx)\ \{\ln (\frac{z + z_0}{z_0}) - \frac{z^2}{2\ H^2}\} +$$

$$+\ u_0{}^2\ \frac{k}{2} \sin\{2(\omega t + kx)\}\ \{\ln (\frac{z + z_0}{z_0}) - \frac{z^2}{2\ H^2}\}^2 +$$

$$-\ u_0{}^2\ \frac{k}{2} \sin\{2(\omega t + kx)\}\ \{\ln (\frac{z + z_0}{z_0}) - \frac{z}{z + z_0} - \frac{z^3}{6\ H^2(z + z_0)} +$$

$$- \frac{z(z + z_0)}{H^2} \ln \left(\frac{z + z_0}{z_0}\right) + \frac{z^2}{H^2} + \frac{z^4}{6\ H^2}\} +$$

$$+ u_0\ k^2\ \varepsilon_x \sin(\omega t + kx)\ \{\ln \left(\frac{z + z_0}{z_0}\right) - \frac{z^2}{2\ H^2}\} +$$

$$- u_0{}^2\ \kappa^2 \sin(\omega t + kx) |\sin\ (\omega t + kx)|$$

$$\{\frac{- 4z}{H^2} + \frac{2\ z(z + z_0)\ (2\ z + z_0)}{H^4} - \frac{2\ z_0}{H^2}\}] \qquad (19a)$$

APPENDIX III: Derivation of the Velocity Profile near the Bottom

Near the bottom the following equation for the horizontal velocity u holds approximately:

$$\frac{\partial}{\partial z} (\varepsilon_z \frac{\partial u}{\partial z}) = c_1 z + c_2 \qquad (20a)$$

Substituting the following mixing length approximation for ε_z into (20a):

$$\varepsilon_z = \kappa^2 (z + z_0)^2 |\frac{\partial u}{\partial z}|, \qquad (21a)$$

and applying the transformation of [1], by which the domain of the problem is transformed into a rectangle, yields:

$$\frac{\partial}{\partial z'} \{k^2 (z' + z_0')^2 |\frac{\partial u}{\partial z'}| \frac{\partial u}{\partial z'}\} TF_3 = \frac{c_1}{TF_3} z' + c_2, \qquad (22a)$$

in which TF_3 is a transfer coefficient, which reads:

$$TF_3 = \frac{1}{\zeta(x,t) - z_b(x)}, \qquad (23a)$$

and in which

$$z_o' = z_o \, TF_3. \qquad (24a)$$

Reordering (22a) yields:

$$\frac{\partial}{\partial z'} \{k^2 (z' + z_0')^2 |\frac{\partial u}{\partial z'}| \frac{\partial u}{\partial z'}\} = c_1' z' + c_2', \qquad (25a)$$

in which:

$$c_1' = \frac{c' - c'_2}{\Delta z} \qquad (26a)$$

$$c' = \left[\frac{\partial u}{\partial t} + \frac{\partial u}{\partial z'} TF_1 + \frac{1}{b} \frac{\partial bu^2}{\partial x} + \frac{\partial u^2}{\partial z'} TF_2 + \frac{\partial uw}{\partial z} TF_3 + \right.$$

$$\left. + \frac{1}{\rho} \frac{\partial p}{\partial x} + \frac{1}{\rho} \frac{\partial p}{\partial z} TF_2 - \varepsilon_x \frac{\partial^2 u}{\partial x^2} \right]_{z=\Delta z} / TF_3 \qquad (27a)$$

$$c_2' = \left[\frac{1}{\rho}\frac{\partial p}{\partial x}\right]_{z'=0} / TF_3 \quad (28a)$$

in which TF_1, TF_2 and TF_3 are transfer coefficients which read:

$$TF_1 = (z - z_b) \frac{(-\frac{\partial \zeta}{\partial t})}{(\zeta - z_b)^2} \quad (29a)$$

$$TF_2 = -\frac{\partial z_b}{\partial x} \frac{1}{(\zeta - z_b)} + (z - z_b) \frac{\{-(\frac{\partial \zeta}{\partial x} - \frac{\partial z_b}{\partial x})\}}{(\zeta - z_b)^2} \quad (30a)$$

$$TF_3 = \frac{1}{\zeta(x,t) - z_b(x)} \quad (31a)$$

Integrating (25a) yields (when primes are ormitted for convenience):

$$\frac{\partial u}{\partial z}\left|\frac{\partial u}{\partial z}\right| = \frac{\frac{c_1}{2} z^2 + c_2 z + c_3}{\kappa^2 (z + z_0)^2} \quad (32a)$$

Now $|c_3| >> |\frac{c_1}{2} z^2 + c_2 z|$ for $0 \leqq z \leqq \Delta z$

So (31a) can be rewritten as:

$$\frac{\partial u}{\partial z} = \frac{(1 + \frac{c_2}{c_3} z + \frac{c_1}{2c_2} z^2)^{\frac{1}{2}}}{\kappa^2 (z + z_0)} \frac{1}{|\frac{\partial u}{\partial z}|} c_3 \frac{(1 + \frac{c_2}{c_3} z + \frac{c_1}{2c_3} z^2)^{\frac{1}{2}}}{(z + z_0)} \quad (33a)$$

$$c_4 = \frac{(1 + \frac{c_2}{c_3} z + \frac{c_1}{2c_3} z^2)^{\frac{1}{2}}}{\kappa^2 (z + z_0)} \frac{1}{|\frac{\partial u}{\partial z}|}$$

and behaves like a constant. Development of the square root into a series of z, (32a) yields:

$$\frac{\partial u}{\partial z} = c_4 \frac{\{\frac{c_1}{4} z^2 + \frac{c_2}{2} z + c_3\}}{(z + z_0)} \quad (34a)$$

in which higher order terms of c_1 and c_2 are neglected.

Integrating (33a) and substituting the boundary condition u = 0 at z = 0 yields:

$$u = c_4 \{\tfrac{1}{2} z^2 + (2 \frac{c_2}{c_1} - z_0)z + (\frac{4c_3}{c_1} - \frac{2c_2}{c_1} z_0 + z_0{}^2)\ln (\frac{z + z_0}{z_0})\}. \quad (35a)$$

Substituting the boundary condition $u = u(\Delta z)$ at $z = \Delta z$ yields c_3:

$$c_3 = \frac{c_1}{c_4} \frac{1}{4 \ln(\frac{\Delta z + z_0}{z_0})} u(\Delta z) - \frac{\{\tfrac{1}{2} c_1 \Delta z^2 + 2c_2 \Delta z - c_1 z_0 \Delta z\}}{4 \ln(\frac{\Delta z + z_0}{z_0})} + $$

$$- c_1 \frac{z_0{}^2}{4} + c_2 \frac{z_0}{2} \quad (36a)$$

Substitution of (35a) into (31a) gives the desired relation for: $\varepsilon_z \frac{\partial u}{\partial z}\Big|_{z= \frac{\Delta z}{2}}$.

APPENDIX IV: Derivation of the Discretisation for $\left|\frac{\partial u}{\partial z}\right|$ near the Bottom

Suppose u can be approximated near the bottom by the following expression:

$$u \;=\; A_1 \ln\left(\frac{z + z_0}{z_0}\right) + A_2 z + A_3 \qquad (37a)$$

then the coefficients A_1, A_2 en A_3 can be found if u(0), u(Δz) and u(2Δz) are known.

This yields:

$$A_1 \;=\; \frac{2\,u(\Delta z) - u(2\Delta z)}{2\ln\left(\frac{\Delta z + z_0}{z_0}\right) - \ln\left(\frac{2\Delta z + z_0}{z_0}\right)} \qquad (38a)$$

$$A_2 \;=\; \frac{u(\Delta z) - A_1 \ln\left(\frac{\Delta z + z_0}{z_0}\right)}{\Delta z} \qquad (39a)$$

$$A_3 \;=\; 0 \qquad (40a)$$

Differentiation of (36a) yields:

$$\frac{\partial u}{\partial z} \;=\; \frac{A_1}{z + z_0} + A_2, \qquad (41a)$$

which expression is used to compute: $\left.\frac{\partial u}{\partial z}\right|_{z=\Delta z}$

APPENDIX V: Discretation of the Free-surface Boundary Condition for the Momentum Equation

The boundary condition for the momentum equation reads:

$$\frac{\partial u}{\partial n} = 0, \tag{1b}$$

which is equivalent to:

$$\frac{\partial u}{\partial x} \left(\frac{\partial \zeta}{\partial x}\right) + \frac{\partial u}{\partial z} = 0. \tag{2b}$$

Applying the coordinate transformation to a rectangular grid yields:

$$\frac{\partial u}{\partial x} \left(\frac{\partial \zeta}{\partial x}\right) + \frac{\partial u}{\partial z} TF_3 \left(1 - \frac{\partial \zeta}{\partial x}\right) = 0 \tag{3b}$$

Rewriting (3b) yields:

$$\frac{\partial u}{\partial z} + \frac{\partial u}{\partial x} \left(\frac{\zeta - z'_b}{TF_3}\right) \frac{\left(\frac{\partial \zeta}{\partial x}\right)}{\left(1 - \frac{\partial \zeta}{\partial x}\right)} = 0 \tag{4b}$$

Discretising (4b) yields:

$$u_{nzz} = u_{nzz-1} - \frac{\Delta z}{\Delta z} \left(\frac{\Delta u}{\Delta z}\right)_{nzz} \frac{1}{(TF_3)_{nzz}} \frac{\left(\frac{\partial \zeta}{\partial x}\right)_{nzz}}{\left(1 - \frac{\partial \zeta}{\partial x}\right)_{nzz}} . \tag{5b}$$

An estimation of the order of magnitude yields:

$$0(u) = 0(u) - \left(\frac{H}{L} \cdot \frac{u}{L} \cdot H \frac{AMPL}{L}\right). \tag{6b}$$

$$\text{Suppose:} \quad \begin{aligned} 0(u) &= 1 \\ 0(n) &= 10 \\ 0(L) &= 1000 \\ 0(AMPL) &= 1, \end{aligned} \tag{7b}$$

substituting (7b) into 6b) yields

$$0(1) = 0(1) - 0(10^{-7}), \tag{8b}$$

which implies that

$$\frac{\partial u}{\partial z} = 0 \tag{9b}$$

is a good approximation of (1b)

APPENDIX VI: Discretisation of the Diffusion Equation, with Truncation Error and Numerical Diffusivity

The differential equation for the diffusion equation reads:

$$\frac{\partial c}{\partial t} + \frac{1}{b}\frac{\partial buc}{\partial x} + \frac{\partial wc}{\partial z} - D_x \frac{\partial^2 c}{\partial x^2} - \frac{\partial}{\partial z}\left(D_z \frac{\partial c}{\partial z}\right) = 0 \tag{1c}$$

For the discretisation of the diffusion equation the same method as for the momentum equation is used, which means that (1c) is spli into a part for the x-direction and a part for the z-direction:

$$\tfrac{1}{2}\frac{\partial c}{\partial t} + \frac{1}{b}\frac{\partial buc}{\partial x} - D_x \frac{\partial^2 c}{\partial x^2} = 0, \tag{2c}$$

$$\tfrac{1}{2}\frac{\partial c}{\partial t} + \frac{\partial wc}{\partial z} - \frac{\partial}{\partial z}\left(D_z \frac{\partial c}{\partial z}\right) = 0. \tag{3c}$$

Now the difference equation read:

$$\frac{(c_{i,j}^{n+\frac{1}{2}} - c_{i,j}^{n})}{\tau} + \frac{\alpha}{b_i}\,\frac{(b_{1+1}\, u_{i+1,j}^{n} c_{i+1,j}^{n} - b_{i-1,j}\, u_{i-1,j}^{n}\, c_{i-1,j}^{n})}{2\,\Delta z}$$

$$+ \frac{(1-\alpha)}{b_i}\,\frac{(b_{i+2}\, u_{i+2,j}^{n}\, c_{i+2,j}^{n} - b_{i-2}\, u_{i-2,j}^{n}\, c_{i-2,j}^{n})}{4\,\Delta x} +$$

$$- D_{x_{ij}}\,\frac{(c_{i+1,j}^{n} - 2c_{i,j}^{n} + c_{i-1,j}^{n})}{\Delta x^2} = 0 \tag{4c}$$

$$\frac{(c_{i,j}^{n+1} - c_{i,j}^{n+\frac{1}{2}})}{\tau} + \frac{(w_{i,j+1}^{n}\, c_{i,j+1}^{n+1} - w_{i,j-1}^{n}\, c_{i,j-1}^{n+1})}{2\,\Delta z} +$$

$$- \frac{\left(\frac{D_{z_{i,j+1}} + D_{z_{i,j}}}{2}\right)\left(\frac{c_{i,j+1}^{n+1} - c_{i,j}^{n+1}}{\Delta z}\right) +}{\Delta z}$$

$$+ \frac{\left(\frac{D_{z_{i,j}} + D_{z_{i,j-1}}}{2}\right)\left(\frac{c_{i,j}^{n+1} - c_{i,j-1}^{n+1}}{\Delta z}\right)}{\Delta z} = 0 \tag{5c}$$

Substitution of $u^{n+1}_{i+1,jn} = e^{\tau L_t} e^{\Delta x L_x} e^{\Delta z L_z} u^n_{i,j}$ etc. into (4c) yields:

$$\frac{(e^{\frac{\tau}{2} L_t} - 1) c^n_{i,j}}{\tau} + \frac{\alpha}{b_i} \{ \frac{(e^{\Delta x L_x} b_i\, e^{\Delta x L_x} u^n_{i,j}\, e^{x L_x} c^n_{i,j})}{2\ \Delta x} + $$

$$- \frac{(e^{-\Delta x L_x} b_i\, e^{-\Delta x L_x} u_{i,j}\, e^{-\Delta x L_x} c^n_{i,j})}{2\ \Delta x}$$

$$+ \frac{(1-\alpha)}{b_i} \{ \frac{(e^{2\Delta x L_x} b_i\, e^{2\Delta x L_x} u^n_{i,j}\, e^{2\Delta x L_x} c^n_{i,j})}{\Delta x} +$$

$$- \frac{(e^{-2\Delta x L_x} b_i\, e^{-2\Delta x L_x} u^n_{i,j}\, e^{-2\Delta x L_x} c^n_{i,j})}{\Delta x} \}$$

$$- D_{x_{i,j}} \frac{(e^{+\Delta x L_x} - 2 + e^{-\Delta x L_x})}{\Delta x^2} c^n_{i,j} = 0 \qquad (6c)$$

Substitution of: $e^{\frac{\tau}{2} L_t} = 1 + \frac{\tau}{2} L_t + \frac{1}{2} (\frac{\tau}{2})^2 L_t^2 + 0(\frac{\tau^3}{2})$ etc. into (6c) yields:

$$\tfrac{1}{2}(L_t + \frac{\tau}{4} L_t^2) c^n_{i,j} + \frac{\alpha}{b_i} \{ \frac{(1 + \Delta x L_x + \frac{\Delta x^2}{2} L_x^2) b_i (1 + \Delta x L_x + \frac{\Delta x^2}{2} L_x^2) u^n_{i,j} (1 + \Delta x L_x + \frac{\Delta x^2}{2} L_x^2) c^n_{i,j}}{2\ \Delta x}$$

$$- \frac{(1 - \Delta x L_x + \frac{\Delta x^2}{2} L_x^2) b_i (1 - \Delta x L_x + \frac{\Delta x^2}{2} L_x^2) u^n_{i,j} (1 - \Delta x L_x + \frac{\Delta x^2}{2} L_x^2) c^n_{i,j}}{2\ \Delta x} \} +$$

$$+ \frac{(1-\alpha)}{b_i} \{ \frac{(1 + 2\Delta x L_x + 4\frac{\Delta x^2}{2} L_x^2) b_i (1 + 2\Delta x L_x + 4\frac{\Delta x^2}{2} L_x^2) u^n_{i,j} (1 + 2\Delta x L_x + 4\frac{\Delta x^2}{2} L^2) c^n_{i,j}}{2\ \Delta x} +$$

$$- \frac{(1 - 2\Delta x L_x + 4\frac{\Delta x^2}{2} L_x^2) b_i (1 - 2\Delta x L_x + 4\frac{\Delta x^2}{2} L_x^2) u^n_{i,j} (1 - 2\Delta x L_x + 4\frac{\Delta x^2}{2} L_x^2) c^n_{i,j}}{4\ \Delta x} \} .$$

$$- D_{x_{i,j}} (L_x^2 + \frac{\Delta x^2}{12} L_x^4) c^n_{i,j} = 0 \qquad (7c)$$

Elaborating (7c) yields:

$$\frac{1}{2}\frac{\partial c}{\partial t} + \frac{1}{b}\frac{\partial buc}{\partial x} - D_x \frac{\partial^2 u}{\partial x^2} = 0 + E_x, \tag{8c}$$

in which E_x is given by:

$$E_x = -\frac{\tau}{8}\frac{\partial^2 c}{\partial t} + \frac{\Delta x^2}{12} D_x \frac{\partial^4 c}{\partial x^4} + 0(\tau^2, \Delta x^4) \tag{9c}$$

By analogy an expression for the truncation error E_z in the z-direction can be derived, which reads:

$$E_z = -\frac{\tau}{8}\frac{\partial^2 c}{\partial t^2} - \frac{\Delta z^2}{2}\{\frac{\partial^2 \omega}{\partial z^2}\frac{\partial c}{\partial z} + \frac{\partial \omega}{\partial}\frac{\partial^2 c}{\partial z^2}\} +$$

$$+ \frac{\Delta z^2}{4}\frac{\partial^2 D_z}{\partial z^2}\frac{\partial^2 c}{\partial z^2} + \frac{\Delta z^2}{6}\frac{\partial D_z}{\partial z}\frac{\partial^3 c}{\partial z^3} + \frac{\Delta z^2}{12} D_z \frac{\partial^4 c}{\partial z^4} + 0(\tau^2, \Delta z^3) \tag{10c}$$

The only term of (9c) that contributes to the numerical diffusivity is:

$$-\frac{\tau}{8}\frac{\partial^2 c}{\partial t}$$

Rewriting of $\frac{\partial^2 c}{\partial t^2}$ yields:

$$\frac{1}{2}\frac{\partial^2 c}{\partial t^2} = \frac{\partial}{\partial t}(-\frac{1}{b}\frac{\partial buc}{\partial x} + D_x \frac{\partial^2 c}{\partial x^2}) =$$

$$= -\frac{1}{b}\frac{b}{\partial x}\frac{\partial uc}{\partial t} - \frac{\partial^2 uc}{\partial x^2 t} + D_x \frac{\partial^3 c}{\partial x^2 \partial t} =$$

$$= -\frac{1}{b}\frac{\partial b}{\partial x}(u\frac{\partial c}{\partial t} + c\frac{\partial u}{\partial t}) - \frac{\partial}{\partial x}(u\frac{\partial c}{\partial t} + c\frac{\partial u}{\partial t}) + D_x \frac{\partial^2}{\partial x^2}(\frac{\partial c}{\partial t}). \tag{11c}$$

Substitution of (2c) into (11c) yields:

$$\frac{1}{2}\frac{\partial^2 c}{\partial t^2} \approx \{-2\frac{u}{b}\frac{\partial b}{\partial x} D_x - \frac{\partial u}{\partial x} D_x + u^2\}\frac{\partial^2 c}{\partial x^2} \quad + \quad \text{higher order terms} \tag{12c}$$

Now the numerical diffusivity reads:

$$D_{nx} = -\frac{\tau}{4}\{u^2 - (2\frac{u}{b}\frac{\partial b}{\partial x} + \frac{\partial u}{\partial x}) D_x\}. \tag{13c}$$

APPENDIX VII: Discretisation of the Diffusion Equation near the Boundaries at $x = 0$ and $x = L$

Because a fourth order scheme is used, difficulties arise by the discretisation at $x = \Delta x$ and at $x = L - \Delta x$, besides the difficulties that already arose at $x = 0$. Therefore a special discretisation is applied at $x = \Delta x$ and $x = L - \Delta x$, which is given in this Appendix.

This discretisation is the second-order-centered difference scheme, which reads:

$$\frac{(c_{i,j}^{n+\frac{1}{2}} - c_{i,j}^{n})}{\tau} + \frac{1}{2\,\Delta x\, b_i}\{b_{i+1}\, u_{i+1,j}^{n}\, c_{i+1,j}^{n} - b_{i-1}\, u_{i-1,j}^{n}\, c_{i-1,j}^{n}\}$$

$$- D_{x_{i,j}} \left\{\frac{c_{i+1,j}^{n} - 2c_{i,j}^{n} + c_{i-1,j}^{n}}{\Delta x^2}\right\} \qquad (14c)$$

The discretisation in the z-direction is identical with (5c).

Analogous to the derivation given in Appendix V. The truncation error of (14c) can be given, which then reads:

$$E_x = -\frac{\tau}{8}\frac{\partial^2 c}{\partial t^2} - \frac{\Delta x^2}{2}\left\{\frac{\partial u}{\partial x} + \frac{u}{b}\frac{\partial b}{\partial x}\right\}\frac{\partial^2 c}{\partial x^2}$$

$$- \frac{\Delta x^2}{2}\left\{\frac{\partial c}{\partial x} + \frac{c}{b}\frac{\partial b}{\partial x}\right\}\frac{\partial^2 u}{\partial x^2}$$

$$- \frac{\Delta x^2}{2}\left\{\frac{u}{b}\frac{\partial c}{\partial x} + \frac{c}{b}\frac{\partial u}{\partial x}\right\}\frac{\partial^2 b}{\partial x^2}$$

$$+ \frac{\Delta x^2}{12} D_x \frac{\partial^4 c}{\partial x^4} + O(\tau^2,\ \Delta x^4). \qquad (15c)$$

The numerical diffusivity is given by:

$$D_{nx} = -\frac{\tau}{4}\{u^2 - (2\frac{u}{b}\frac{\partial b}{\partial x} + \frac{\partial u}{\partial x})D_x\} - \frac{\Delta x^2}{2}\{\frac{\partial u}{\partial x} + \frac{u}{b}\frac{\partial b}{\partial x}\}. \qquad (16c)$$

The truncation error at $x = o$ reads:

$$E_x = -\frac{\tau}{8}\frac{\partial^2 c}{\partial t^2} + O(\tau^2, \Delta x^3) \qquad (17c)$$

And the numerical diffusivity is given by:

$$D_{nx} = -\frac{\tau}{4}\{u^2 - (2\frac{u}{b}\frac{\partial b}{\partial x} + \frac{\partial u}{\partial x})D_x\} \qquad (18c)$$

p.o. box 177 delft the netherlands